Supplementary Information

A phase transfer-assisted strategy for oxidation based biomass valorization

Junhao Wang,[a] Baoyin An,[a] Pengfei Li,[a] Huili Zhang[a] and Yunming Fang*[a]

a. State Key Laboratory of Green Biomanufacturing, Beijing University of Chemical Technology, Beijing 100029, P.R. China. E-mail: fangym@mail.buct.edu.cn

Table of Content

Chemical and Materials

Tetrabutylammonium bromide (TBAB, 98%), acetylcholine chloride (Ach, 98%), alpha-cyclodextrin (α-CD, > 98%), tetrabutylammonium hydroxide (TBAH, > 97%), trimethyl glycine (TMG, 97%), vanillin (> 98%), acetovanillone (98%), vanillin acid (98%), 4-hydroxyacetophenone (98%), syringaldehyde (98%) were purchased from TCI. Xylan (95%), α-cellulose (particle size: 250 μm), guaiacol (99%), sodium sulfate (99%) and sodium hydroxide (99%) were purchased from Macklin. 1-(4-Hydroxy-3,5-dimethoxyphenyl)-2-(2-methoxyphenoxy)propane-1,3-diol (98%), ferulic acid (98%), dehydrodiconiferyl alcohol (98%) and pinoresinol (95%) were purchased from Bidepharm. 4-hydroxy benzaldehyde (98%), tetrahydrofuran (> 99.8%), ethyl acetate (EtOAc, 99%) and methanol (99.9%) were purchased from Alfa Aesar. Formic acid (≥ 96%), acetic acid (≥ 99%), oxalic acid (≥ 99%), lactic acid (≥ 85%), tartronic acid (99%), glycolic acid (70wt.% in H_2O), gluconic acid (97%), succinic acid (≥ 99%) and manlonic acid (99%) were purchased from Sigma-Aldrich. All commercial chemicals were used without purification. Water was purified using a Millipore Milli-Q Advantage A10 water purification system to a resistivity higher than 18 MΩ.cm.

The pine wood comes from the Songhua River Basin in China. It is crushed into 40-60 mesh particles and then extracted with a mixture of ethanol and toluene (1:1) for 24 hours. Once cooled to room temperature, samples were washed with hexane and dried in a vacuum oven at 80 °C.

The pine-milled wood lignin (Pine-MWL) preparation process

16 g of pine wood raw material and a certain proportion of grinding balls (φ10-large 20 wt%, φ6-medium 50 wt%, φ2-small 30 wt%) were placed in a planetary ball mill at 500 rpm for 10 min, with an interval of 5 min, and continuous ball milling for 18 hours. The pH was adjusted to 4.8 with 0.1 M NaOH solution. After the ball milled sample was collected with 100 ml of pH 4.8 citric acid buffer solution, it was mixed with 1.5 ml of cellulase, 1.5 ml of xylanase and 150 ml of pH 4.8 citric acid buffer solution and shaken at 50 °C and 180 rpm for 24 hours. The enzymatic hydrolysis sample was centrifuged and repeatedly washed with deionized water until neutral and freeze-dried at -80 °C for 3 days. The freeze-dried sample was mixed with 300 ml of 1,4-dioxane and shaken at 35 °C and 180 rpm in a dark environment for 24 hours for lignin extraction. After the extraction, the filtrate was filtered with an organic membrane and evaporated to 5 ml using a rotary evaporator at 50 °C. After the concentrate was mixed with 50 ml of deionized water, lignin was rapidly precipitated and then placed in a refrigerator for 12 hours for precooling. After freeze drying at -80 °C for 4 days, Pine-MWL was obtained.

Alkaline oxidative depolymerization (AOD) of biomass sawdust

In the typical experiment, pine sawdust (0.4 g, 40-60 mesh), NaOH (2.25 g, 7.5 wt%), phase transfer catalyst (0.75 g, 2.5 wt%) and deionized water (30 ml) were charged into the 50 ml stainless steel reactor (Parr Instruments & Co.). The reactor was purged with N_2 to remove air, and then was pressurized with O_2 to the 0.4 Mpa at room temperature. The reaction mixture was heated to 160 °C and kept for 40 min under a certain agitation speed of 500 rpm. Afterwards, the reactor was cooled and depressurized at room temperature and thoroughly rinsed with 30 ml of deionized water to transfer the products. The soluble fraction and solid phase were separated through filtration with a 0.22 μm filter. The soluble fraction was acidified to pH of 5.0 with HCl to precipitate the oxygenated aromatic compounds and lignin fragments. The precipitated products were extracted with EtOAc (10 × 10 ml) to obtain an organic phase containing aromatic aldehydes and an aqueous phase containing small molecular aliphatic acids. The substance obtained by thoroughly removing the solvent from the organic phase is called AOD oil. Lignin fragments were separated through filtration for further research.

HSQC NMR analysis

All NMR spectral data reported in this study were recorded with a Bruker Avance/DMX 400 MHz NMR spectrometer and were provided technical support by "Ceshigo Research Service, (www.ceshigo.com)". 2D heteronuclear single quantum coherence (HSQC NMR) spectra were acquired using approximately 70 mg of Pine-MWL and lignin fragments dissolved in 450 μl of dimethylsulfoxide-d_6 (DMSO-d_6), employing a standard Bruker pulse sequence "hsqcetgpsi.2" with a 90° pulse, 0.11 s acquisition time, 1.5 s pulse delay, 1JC-H of 145 Hz, 48 scans, and acquisition of 1024 data points (for ^{1}H) and 256 increments (for ^{13}C). The central solvent peak was used for chemical-shift calibration. HSQC NMR spectra processing and plots were performed using the default processing template, automatic phase, and baseline correction of TopSpin software (v4.4.0).

The semi-quantitative analysis methods of the HSQC NMR spectra for the correlation peaks in different spectra regions were summarized in Table S6. The relative quantity of side chains involved in the interunit linkages and lignin end-groups was expressed as a number per 100 C_9 units (total aromatic content), as shown in the Table S6. Assignments of main ^{13}C-^{1}H crosslinking signals in the HSQC NMR spectra were shown in Table S10.

Qualitative and quantitative analysis of phenolic compounds

Analysis of monomers: To analyze lignin monomers in the AOD oil, 1 ml of ethyl acetate extract phase after dehydration with anhydrous sodium sulfate for analysis. Quantitative analysis of lignin monomers was performed with GC (Shimadzu 2030) system equipped with an Agilent HP-5 MS column (30 m × 0.25 mm × 0.25 μm) and a flame ionization detector (FID). The column temperature program was: 40 °C (5 min), ramping of 10 °C min^{-1} to 280 °C (6 min). The SPL injection port temperature and FID temperature were both 300 °C. Quantitative analysis of lignin monomers was performed with GC-MS (Shimadzu 2010SE) system equipped with an Agilent HP-5 MS column (30 m × 0.25 mm × 0.25 μm) and a mass spectrometer detector. The column temperature program and SPL injection port temperature are the same as above. The MSD transfer line temperature and the EI ion source temperature were 280 °C and 230 °C, respectively. Yield and selectivity were calculated based on the calibration curves established on the dependency of the chromatographic areas as a function of concentration (Fig. S24). The detailed calculations were as follows:

$$C_{\mathrm{lignin}} = \frac{W_{\mathrm{Klason\ lignin}} - W_{\mathrm{AOD\ oil}}}{W_{\mathrm{Klason\ lignin}}} \times 100\% \tag{S1}$$

$$Y_{\mathrm{lignin\ monomer}} = \frac{W_{\mathrm{lignin\ monomers\ in\ sample}} \times V}{W_{\mathrm{Klason\ lignin\ in\ pine}}} \times 100\% \tag{S2}$$

$$S_{\mathrm{lignin\ monomer}} = \frac{Y_{\mathrm{lignin\ monomer}}}{Y_{\mathrm{total\ lignin\ monomers}}} \times 100\% \tag{S3}$$

In these formulas,
C_{lignin}: the conversion rate of the lignin in pine wood
$W_{\mathrm{Klason\ lignin}}$: the weight of the Klason lignin in pine wood
$W_{\mathrm{AOD\ oil}}$: the weight of AOD oil
$Y_{\mathrm{lignin\ monomer}}$: the yield of lignin monomers
V: the volume of EtOAc phase (approximately 96 ml, because about 4 ml of EtOAc is slightly soluble in the aqueous phase)
$S_{\mathrm{lignin\ monomer}}$: the selectivity of a lignin monomer

Analysis of dimers: In order to analyze the non-volatile lignin dimers in the AOD oil, the sample needs to be derivatized. Derivatization was performed as described previously.[1] In short, 50 mg dried AOD oil samples, 0.5 ml of anhydrous pyridine, and 0.5 ml of N-methyl-N-(trimethylsilyl)trifluoroacetamide (MSTFA) was added into GC-vial. The vial was sealed and put in an oven at 80 °C for 30 min. The vial was removed from the oven and cooled to room temperature before being injected on the GC-MS.

The inlet temperature of the GC-MS was 330 °C. The oven was programmed to ramp from 50 °C to 330 °C at a rate of 10 °C min^{-1} and held at 330 °C for 7 min. The solution was analyzed with a GC-MS (Shimadzu 2010SE) system equipped with an Agilent HP-5 MS column (30 m × 0.25 mm × 0.25 μm) and a mass spectrometer detector. Six lignin dimers were inferred by analyzing the mass spectrometry peaks, which were located in the region with retention times between 17 and 27 minutes in the TIC spectrum (Fig. S19d).

The determination method of the Klason lignin in pine wood according to the NREL[2]

Take 0.2 g of the raw material and place it in a beaker. Add 3 ml of 72 wt% sulfuric acid and mix well. After stirring for 2 hours, it was diluted with water until the acid concentration was 4 wt%. Then place it in a 121 °C environment and react for 1 hour. After cooling, filter the mixture and dry the obtained black solid in a 105 °C oven for 12 hours. After cooling, weigh it to obtain the Klason lignin content.

Qualitative and quantitative analysis of aliphatic acids

Analysis of aliphatic acids in EtOAc phase: To qualitative analyze of aliphatic acids, the GC-MS analysis method for lignin dimers mentioned above was used. Peaks with retention time between 7 and 12 minutes in the TIC spectrum (Fig. S19c) were matched to 10 aliphatic acids through NIST17 MS libraries comparison.

Analysis of aliphatic acids in aqueous phase: Quantitative analysis of aliphatic acids in the aqueous phase was performed by HPLC (Shimadzu LC-20A), equipped with a RID detector. The accuracy of the aliphatic acids matched by GC-MS characterization was determined by comparing the retention time of the peaks in the HPLC spectra. Aliphatic acid concentration in aqueous phase was calculated based on the calibration curves established on the dependency of the chromatographic areas as a function of concentration (Fig. S25).

Gel permeation chromatography (GPC) analysis

GPC analysis of the AOD oil and lignin fragments was performed using the Agilent PLgel MIXED-E (300 × 7.5 mm, 3 μm) and the Agilent PLgel MIXED-C (300 × 7.5 mm, 5 μm) chromatography columns, respectively, at 330 nm and 248 nm detection wavelengths (Shimadzu LC-20A, equipped with UV-Vis detector). The column was calibrated with polystyrene standards (M_w: 266-62500 Da). Analysis was carried out at 25 °C using THF as eluent with a flow rate of 1 ml min^{-1}. Samples were prepared with a concentration of 2 mg ml^{-1}, and filtered using 0.45 μm filter membrane prior to test.

AOD reaction kinetics calculation method

The depolymerization of lignin in the batch reactor mainly includes two processes:

- I. Sodium hydroxide acts as a catalyst to promote the lignin cracking reaction on the surface of the unreacted core of the solid phase lignin particles, which is the chemical reaction process.
- II. The depolymerization products diffuse from the unreacted core surface of the lignin particles to the main body of the fluid through the liquid film, which is the liquid film mass transfer process.

Basic assumptions of the model:

- I. The lignin particles are dense and non-porous.
- II. The lignin particles are irregular and approximately spherical.
- III. The particle size of the lignin particles is constantly decreasing during the reaction.
- IV. The depolymerization of lignin is a heterogeneous reaction, and the reaction is limited to the particle surface.
- V. The temperature fluctuation during the depolymerization process is negligible.

Chemical Reaction Process

Previous studies have shown that the depolymerization of lignin in an intermittent reaction vessel is a first-order irreversible reaction[3-5], and the reaction rate formula is:

$$\frac{\mathrm{d}X}{\mathrm{d}t} = k_{\mathrm{S}}(1 - X) \tag{S11}$$

As the reaction time changes from 0 to t, the conversion rate changes from X_0 to X, and the integral formula (S11) yields:

$$\int_{X_0}^{X} \frac{\mathrm{d}X}{1-X} = \int_{0}^{t} k_\mathrm{S}\,\mathrm{d}t \tag{S12}$$

Since k_S is a constant, further integrating formula (S12) yields:

$$t = \frac{1}{k_\mathrm{S}} \ln \frac{1-X_0}{1-X} \tag{S13}$$

According to Arrhenius's law:

$$k_\mathrm{S} = A_\mathrm{S} e^{-E_\mathrm{S}/RT} \tag{S14}$$

Taking the logarithm of formula (S14) can get:

$$\ln k_\mathrm{S} = \ln A_\mathrm{S} - \frac{E_\mathrm{S}}{RT} \tag{S15}$$

Combining formula (S13) and (S14) can get the kinetic formula of the chemical reaction process:

$$t = \frac{1}{A_\mathrm{S}} e^{E_\mathrm{S}/RT} \ln \frac{1-X_0}{1-X} \tag{S16}$$

In the formula above: X is the conversion rate of lignin, %; t is the reaction time, min; k_S is the chemical reaction rate constant, min^{-1}; X_0 is the conversion rate of lignin at the initial moment, %; A_S is the pre-exponential factor; E_S is reaction activation energy, kJ mol^{-1}; R is the molar gas constant, the value is 8.314 J $(\mathrm{mol{\cdot}K})^{-1}$; T is the reaction temperature, K.

It can be seen from formula (S15) that $\ln k_\mathrm{S}$ and $1/T$ are linearly related, with a slope of $-E/R$ and an intercept of $\ln A$. Therefore, $\ln k_\mathrm{S}$ and $1/T$ can be linearly fitted (Fig. S15a and 15b), and then calculate the pre-exponential factor A_S and the reaction activation energy E_S, thereby determining the kinetic formula of the chemical reaction process.

The kinetic formula of the AOD of pine wood without adding TBAB:

$$t = 32.14\, e^{458.35/RT} \ln \frac{1-X_0}{1-X} \tag{S17}$$

The kinetic formula of the AOD of pine wood with TBAB:

$$t = 24.53\, e^{362.20/RT} \ln \frac{1-X_0}{1-X} \tag{S18}$$

Liquid Film Mass Transfer Process

Relationship between the amount of substance and time during lignin depolymerization:

$$-\frac{\mathrm{d}n_\mathrm{A}}{\mathrm{d}t} = -\frac{\mathrm{d}}{\mathrm{d}t}\left(\frac{\rho}{M_\mathrm{A}} \frac{4}{3} \pi R_\mathrm{C}^3\right) = -\frac{4\pi R_\mathrm{C}^2 \rho}{M_\mathrm{A}} \frac{\mathrm{d}R_\mathrm{C}}{\mathrm{d}t} \tag{S19}$$

Mass transfer rate of depolymerization products through liquid film:

$$-\frac{\mathrm{d}n_\mathrm{A}}{\mathrm{d}t} = 4\pi R_\mathrm{C}^2 k_\mathrm{L} \left(C_{\mathrm{B_S}} - C_{\mathrm{B_L}}\right) \tag{S20}$$

Relationship between lignin and depolymerization products:

$$\frac{\mathrm{d}n_\mathrm{A}}{\mathrm{d}t}=\frac{M_\mathrm{B}}{M_\mathrm{A}}\frac{\mathrm{d}n_\mathrm{B}}{\mathrm{d}t} \tag{S21}$$

The combination of formula (S19), (S20) and (S21) can be obtained:

$$-\frac{\mathrm{d}R_\mathrm{C}}{\mathrm{d}t}=\frac{M_\mathrm{A}}{\rho}k_\mathrm{L}\left(C_{\mathrm{B_S}}-C_{\mathrm{B_L}}\right) \tag{S22}$$

Relationship between lignin conversion rate *X* and R_C:

$$X=1-\left(\frac{R_\mathrm{C}}{R_0}\right)^3 \tag{S23}$$

The molar concentration of the depolymerization product outside the liquid film is:

$$C_{\mathrm{B_L}}=\frac{mX}{M_\mathrm{B}V} \tag{S24}$$

The molar concentration of the depolymerization products on the surface of lignin particles is:

$$C_{\mathrm{B_S}}=\frac{\rho}{M_\mathrm{B}} \tag{S25}$$

Substitute formula (S24) and (S25) into formula (S22) to get:

$$-\frac{\mathrm{d}R_\mathrm{C}}{\mathrm{d}t}=\frac{M_\mathrm{A}}{\rho}k_\mathrm{L}\left(\frac{\rho}{M_\mathrm{B}}-\frac{mX}{M_\mathrm{B}V}\right) \tag{S26}$$

From reaction time 0 to *t*, particle radius R_P to R_C, the integral formula (S26) is:

$$k_\mathrm{L}t=\frac{\rho M_\mathrm{B}VR_0\left[(1-X_0)^{\frac{1}{3}}-(1-X)^{\frac{1}{3}}\right]}{M_\mathrm{A}(\rho V-mX)} \tag{S27}$$

In order to facilitate the calculation of formula (S27), the product of the liquid film mass transfer coefficient k_L and the reaction time *t* is *P*:

$$P=\frac{\rho M_\mathrm{B}VR_0\left[(1-X_0)^{\frac{1}{3}}-(1-X)^{\frac{1}{3}}\right]}{M_\mathrm{A}(\rho V-mX)} \tag{S28}$$

According to Arrhenius's law:

$$k_\mathrm{L}=A_\mathrm{L}e^{-E_\mathrm{L}/RT} \tag{S29}$$

Taking the logarithm of both sides of formula (S24) gives:

$$\ln k_\mathrm{L}=\ln A_\mathrm{L}-\frac{E_\mathrm{L}}{RT} \tag{S30}$$

Combining formula (S27) and (S29), the kinetic formula of the liquid film mass transfer process is obtained:

$$t = \frac{1}{A_{\mathrm{L}}} e^{E_{\mathrm{L}}/RT} \frac{\rho M_{\mathrm{B}} V R_0 \left[(1 - X_0)^{\frac{1}{3}} - (1 - X)^{\frac{1}{3}}\right]}{M_{\mathrm{A}}(\rho V - mX)} \tag{S31}$$

In the formula: n_A and n_B are the amounts of lignin and depolymerization products respectively, mol; M_A and M_B are the molar mass of lignin and depolymerization products respectively, where M_A is 10233 g mol^{-1}; R_P and R_C are the particle radius when the reaction time is 0 and t respectively, cm; k_L is the mass transfer coefficient of the depolymerization product in the liquid film, cm^2 min^{-1}; C_{Bs} and C_{BL} are the molar concentration of the depolymerization products outside the liquid film and on the particle surface, mol cm^{-3}, respectively; R_0 is the initial radius of the particle, which is 0.0046 cm; m is the total mass of the lignin, which is 0.1152 g; ρ is the lignin density, which is 1.33 g cm^{-3}; V is the volume of the reactor, which is 50 ml.

According to formula (S30), lnk_L and $1/T$ are also linearly fitted to calculate the pre-exponential factor A_L and the reaction activation energy E_L (Fig. S18c, d), thereby determining the kinetic formula of the liquid film mass transfer process.
The kinetic formula of the AOD of pine wood without adding TBAB:

$$t = 420485.05\, e^{98.97/RT} \frac{M_{\mathrm{B}} \left[(1 - X_0)^{\frac{1}{3}} - (1 - X)^{\frac{1}{3}}\right]}{(66.50 - 0.1152X)} \tag{S32}$$

The kinetic formula of the AOD of pine wood with TBAB:

$$t = 749303.96\, e^{39.09/RT} \frac{M_{\mathrm{B}} \left[(1 - X_0)^{\frac{1}{3}} - (1 - X)^{\frac{1}{3}}\right]}{(66.50 - 0.1152X)} \tag{S33}$$

a With TBAB

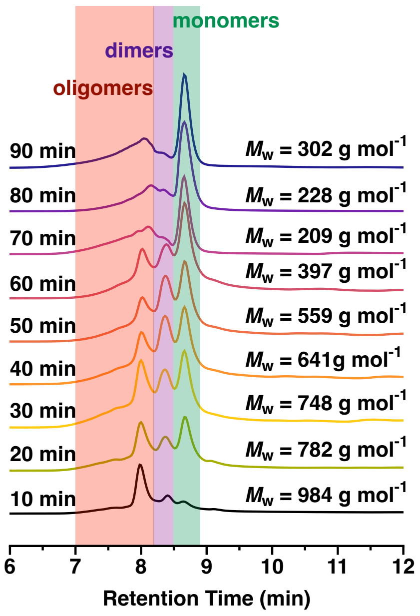

b None

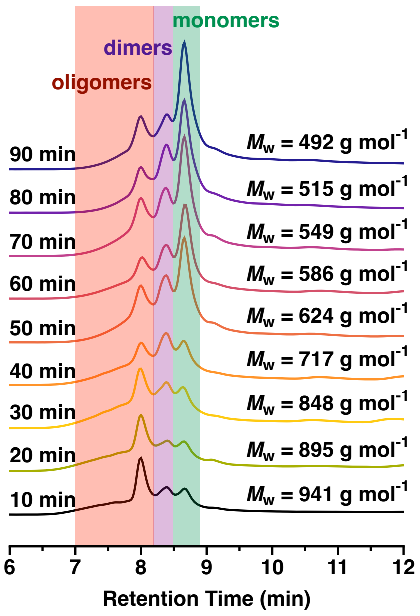

Fig. S1. GPC spectra of the AOD oil at different reaction times. (a) Reaction with TBAB, (b) Reaction without adding TBAB. Reaction conditions: 0.4 g pine, 7.5 wt% NaOH, 2.5 wt% TBAB or no addition, 160 °C, 60 min, 500 rpm, 0.4 Mpa O_2

a With TBAB

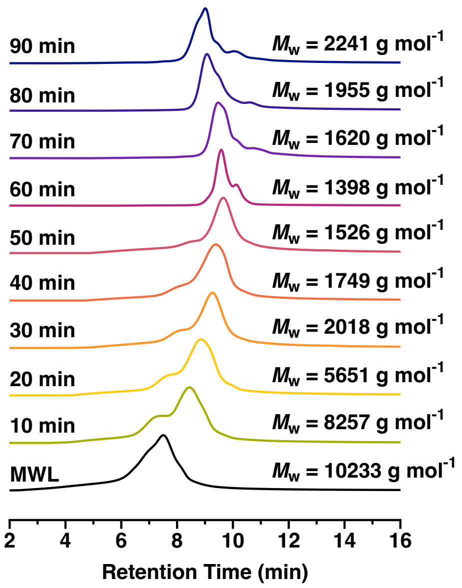

b None

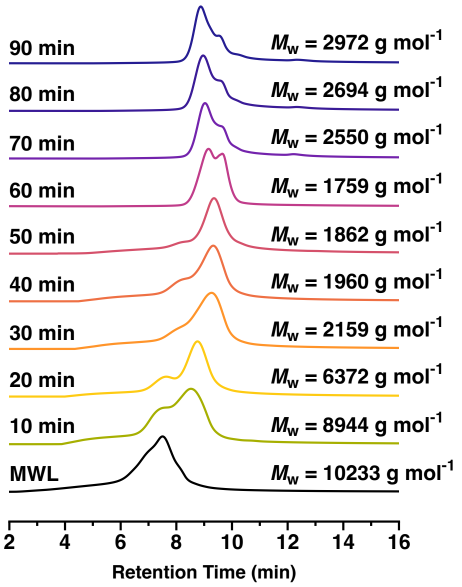

Fig. S2. GPC spectra of the lignin fragments at different reaction times. (a) Reaction with TBAB, (b) Reaction without adding TBAB. Reaction conditions: 0.4 g pine wood, 7.5 wt% NaOH, 2.5 wt% TBAB or no addition, 160 °C, 60 min, 500 rpm, 0.4 Mpa O_2.

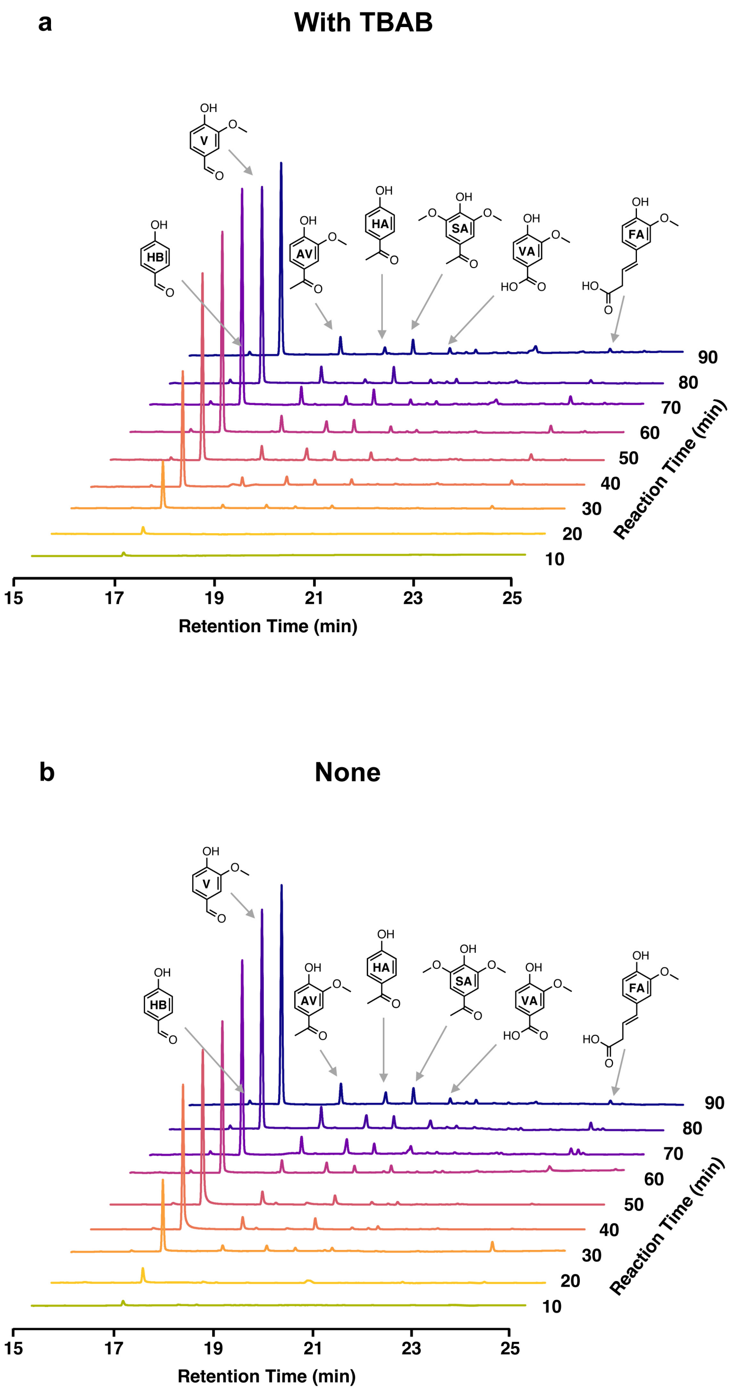

Fig. S3. GC spectrum of the organic phase product. (a) The AOD of pine wood with TBAB, (b) AOD of pine wood without adding TBAB. Reaction conditions: 0.4 g pine wood, 7.5 wt% NaOH, 2.5 wt% TBAB or no addition, 160 °C, 60 min, 500 rpm, 0.4 Mpa O_2.

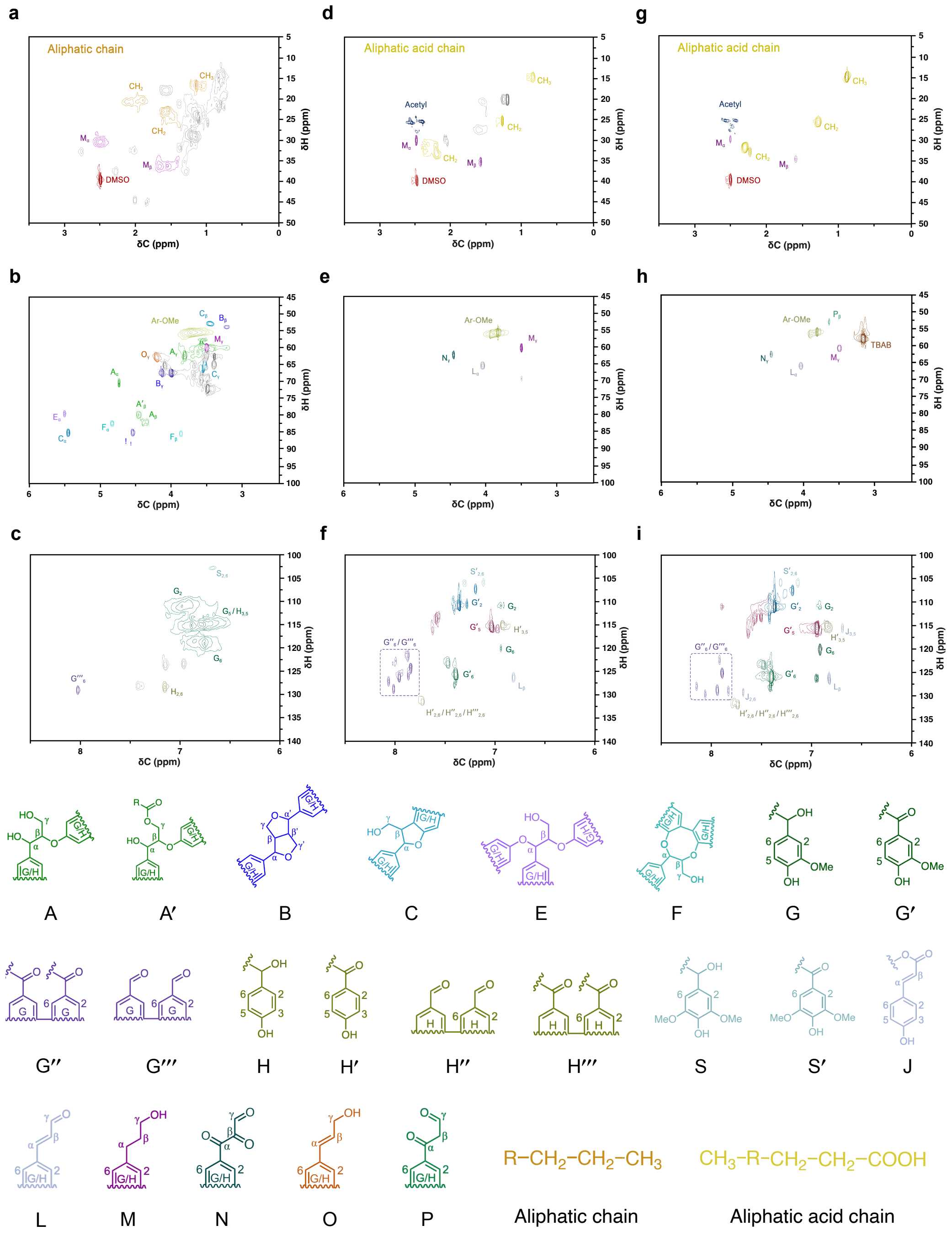

Fig. S4. HSQC spectra. (a-c) The Pine-MWL, (d-f) The AOD oil obtained by reaction without adding TBAB, (g-i) The AOD oil obtained by reaction with TBAB.

Supplementary Note 1

Less substructure N and M existed in the presence of TBAB as more lignin was oxidized to benzaldehydes. Barely no cross-linking signal appeared in this interlinkage region except for that of the methoxyl (δ_C/δ_H = 55.64/3.79 ppm). Therefore, the lignin units in oligomers were most likely linked by C−C (aliphatic or Caryl−Caryl-like 5−5) bonds. The aromatic region (δ_C/δ_H = 100−140/6−8.5 ppm), shows the oxidized G units (G′, G″, and G‴) dominant signals with a few signals of the oxidized hydroxyphenyl units (H′, H″, and H‴) analogues at the expense of G and H units, revealed the effective oxidation.

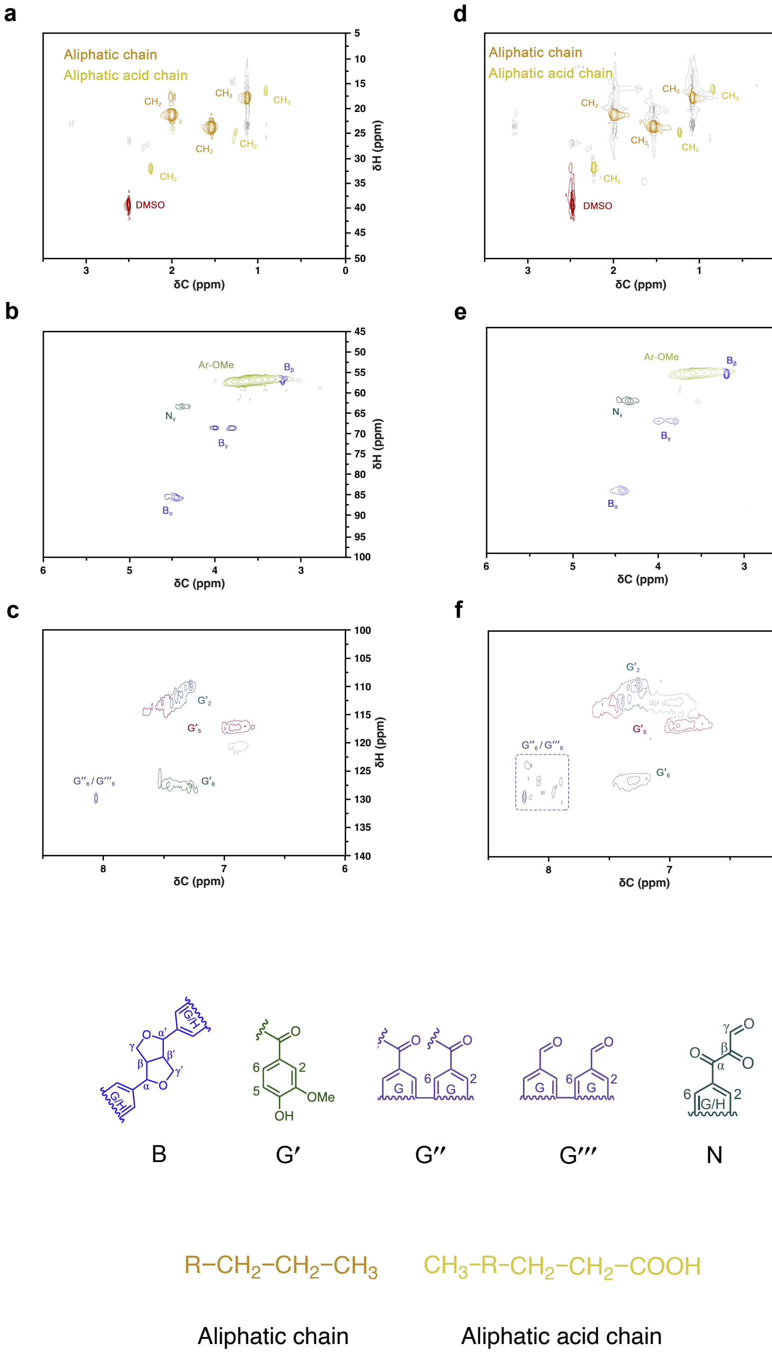

Fig. S5. HSQC spectra. (a-c) the lignin fragments obtained by reaction without adding TBAB, (d-f) the lignin fragments obtained by reaction with adding TBAB.

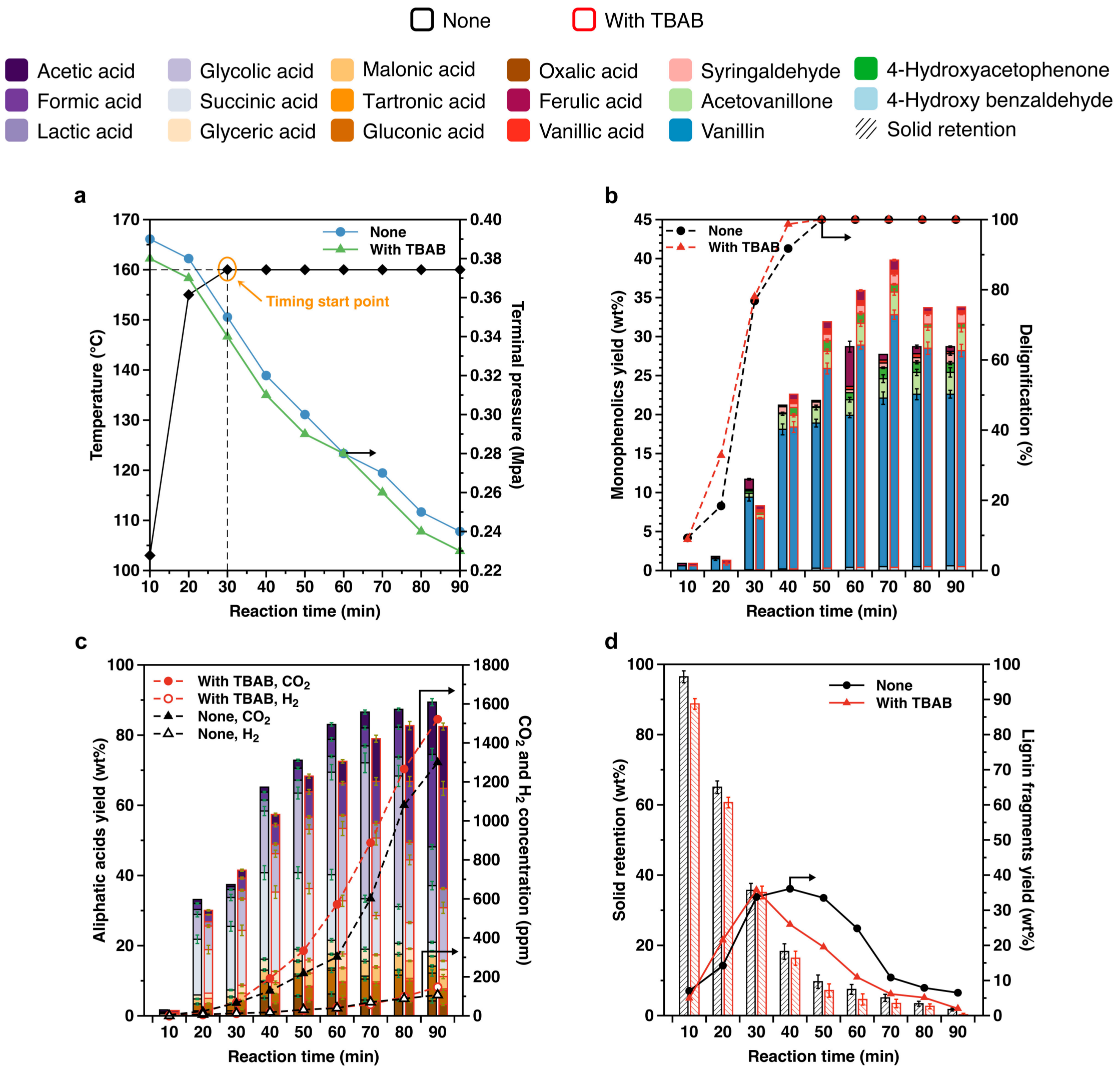

Fig. S6. The AOD of pine wood: effects of reaction time on the reactor temperature and terminal pressure (a), the monophenolics yield and delignification (b), the aliphatic acids yield and CO_2 and H_2 concentration (c) and the SR and lignin fragments yield (d). Reaction conditions: 0.4 g pine wood, 7.5 wt% NaOH, 2.5 wt% TBAB, 160 °C, 60 min, 500 rpm, 0.4 Mpa O_2.

Supplementary Note 2

The timing started when the temperature reached 160 °C. The first 30 minutes were the heating time, so the data recording time was 90 minutes.

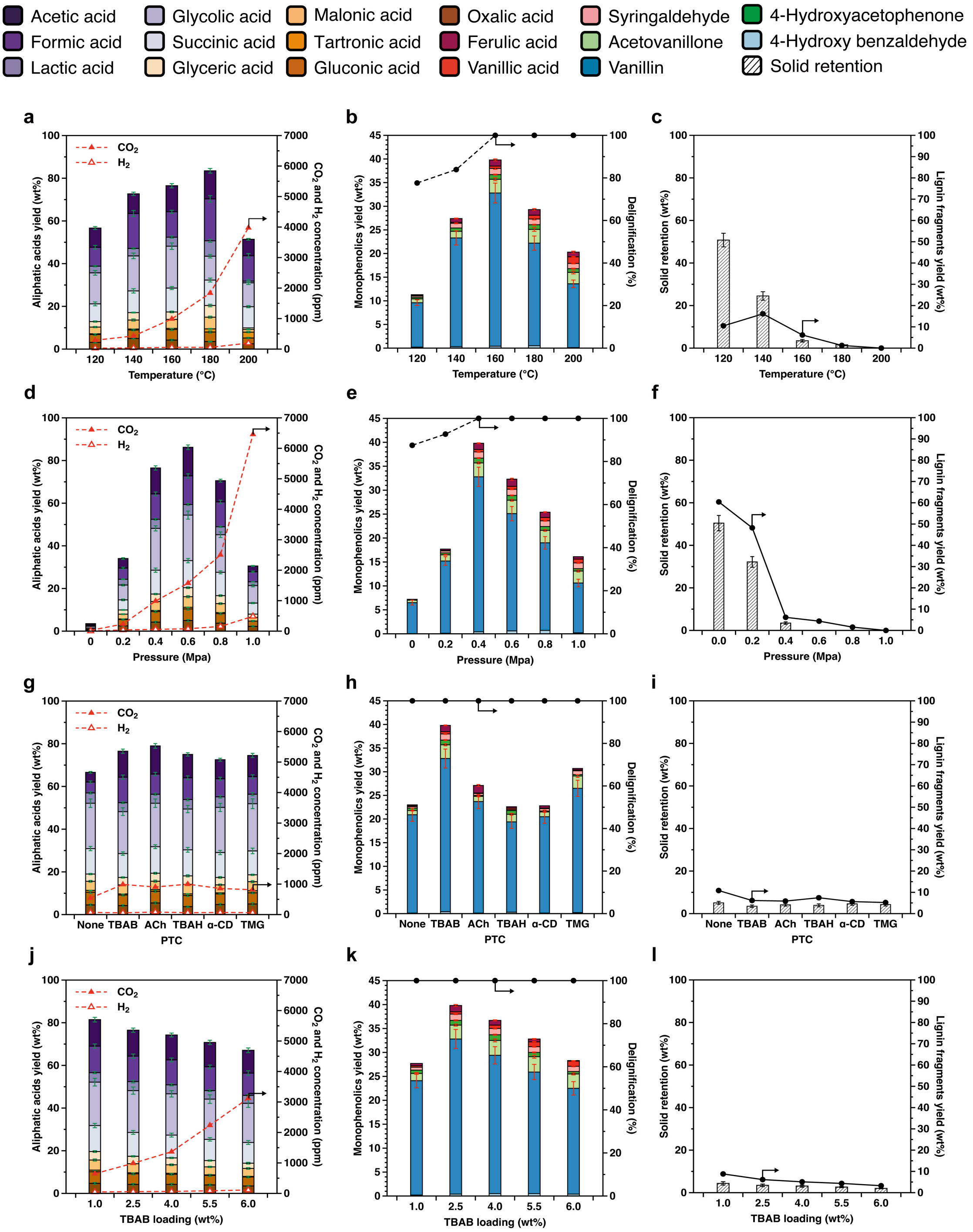

Fig. S7. The AOD of pine wood: effects of temperature (a-c), pressure (d-f), PTC substances (g-i), and loading of TBAB (j-l) on the yields of aliphatic acids, monophenolics, solid retention (SR) and lignin fragments, CO_2 and H_2 concentration, and delignification. Reaction conditions: 0.4 g pine wood, 7.5 wt% NaOH, 40 min, 500 rpm.

Supplementary Note 3

Carbon dioxide originates from excessive oxidation of biomass. The hydrogen may be produced by the methoxyl radicals (•OCH_3) released during the depolymerization of lignin. These radicals react with oxygen to form formaldehyde, which is then further oxidized to sodium formate under alkaline condition and then decomposed by heat.[6]

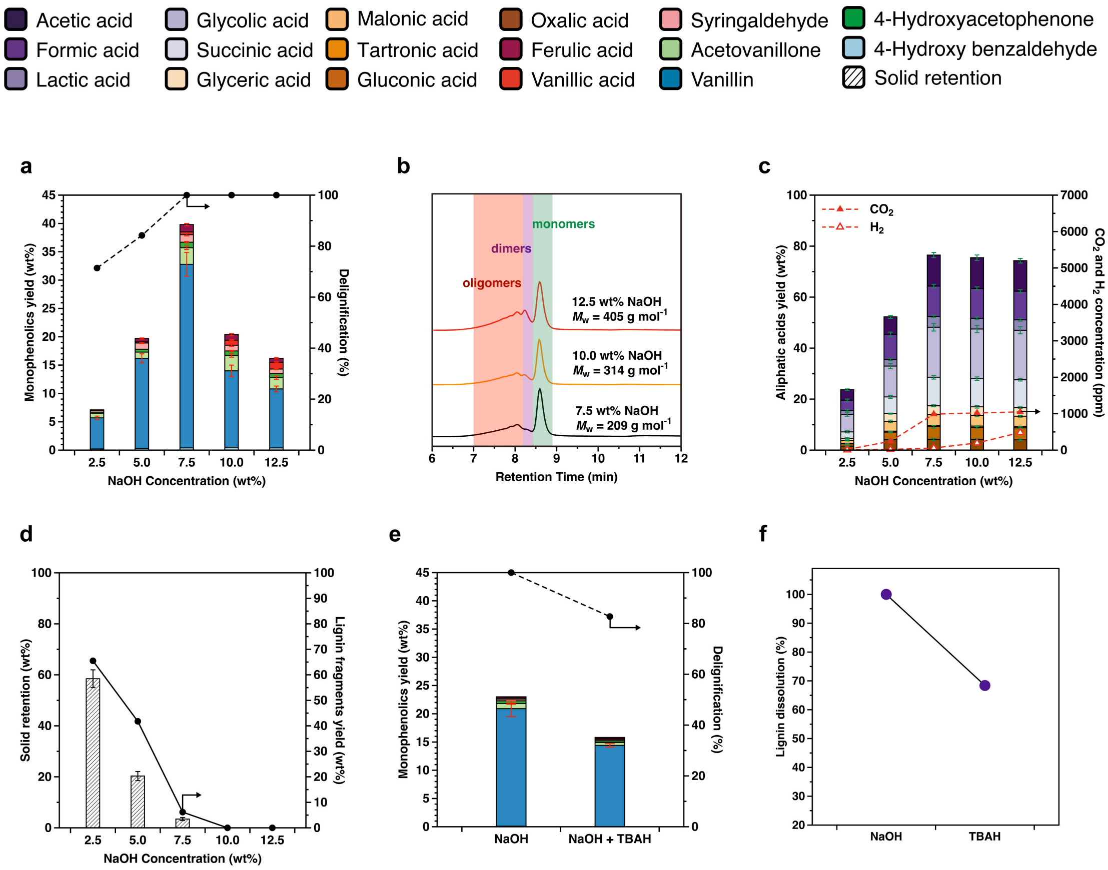

Fig. S8. The AOD of pine wood: effects of alkaline concentration (a-d), (e) TBAH replaces part of NaOH on pine wood depolymerization, (f) Effects of NaOH and TBAH on the lignin dissolution. Reaction conditions in Fig. S9a-d: 0.4 g pine wood, 2.5 wt% TBAB, 160 °C, 40 min, 500 rpm, 0.4 Mpa O_2. Reaction conditions in Fig. S9e: 0.4 g pine wood, 56 mmol (7.5 wt%) NaOH or 28 mmol NaOH with 28 mmol TBAH, 30 ml water, 160 °C, 40 min, 500 rpm, 0.4 Mpa O_2.

Supplementary Note 4

1) We evaluated TBAB's basicity by measuring the pH of 0.5 M TBAB and 0.5 M NaOH aqueous solutions at 25 °C, which were 13.5 and 12.9, respectively, indicating that TBAB behaves as a comparably strong base under these conditions. However, when the total NaOH concentration is increased beyond optimal levels, vanillin undergoes self-condensation, thereby reducing its monomeric yield (Fig. S8a), in agreement with Ma *et al.*[7] This side reaction is further supported by gel-permeation chromatography of the AOD oil, which shifts toward higher molecular weights at elevated hydroxyl (OH^-) concentration (Fig. S8b).

2) In addition, We also examined how alkali concentration influences (i) the formation of aliphatic acids, (ii) the CO_2 and H_2 composition of the off-gas (Fig. S8c), (iii) solid residue yield, and (iv) the distribution of lignin fragments (Fig. S8d).

3) To probe the specific role of the tetrabutylammonium cation, we replaced a portion of NaOH with TBAH while maintaining a constant [OH^-]. As shown in Fig. S8e, this

substitution led to lower lignin monomer yields despite identical hydroxide levels. Dissolution tests with industrial alkali lignin in NaOH versus TBAH solutions revealed that only 68.4 wt% of lignin dissolved in the latter (Fig. S8f). We attribute this diminished solubility and the concomitant poorer depolymerization performance on pine wood to the steric bulk of the tetrabutylammonium cation, which hinders its electrostatic interaction with the phenolic-O^- sites of lignin and thus limits lignin solubilization under alkaline conditions.

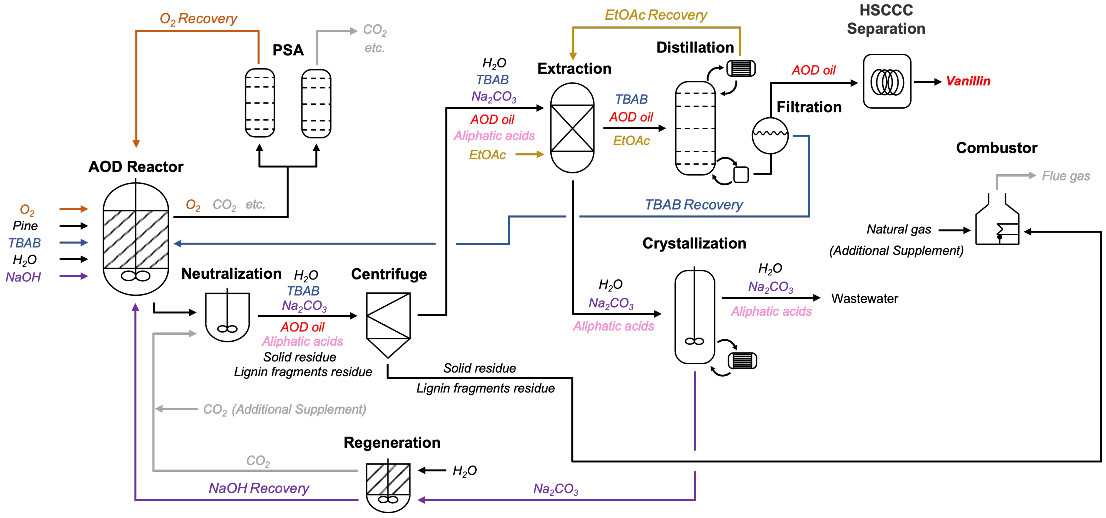

Fig. S9. The proposed block flow diagram of the biorefinery to produce vanillin from pine wood.

Supplementary Note 5

In the AOD process, high-purity vanillin is achieved through a series of separation processes, including neutralization, centrifugation, extraction, distillation (for EtOAc recovery), and high-speed counter current chromatography (HSCCC). Following multi-extraction, TBAB is enriched in the organic phase. After EtOAc is recovered, the AOD oil and TBAB can be separated by filtration. Sodium carbonate (used for sodium hydroxide regeneration) in the aqueous phase is recovered by crystallization, yielding an aqueous solution rich in aliphatic acids, which is then fed into the wastewater treatment plants. Oxygen required for the reactions are recovered by the pressure swing adsorption (PSA) unit. The natural gas along with the SR and LF form the AOD process, are sent to the boiler for heat generation.

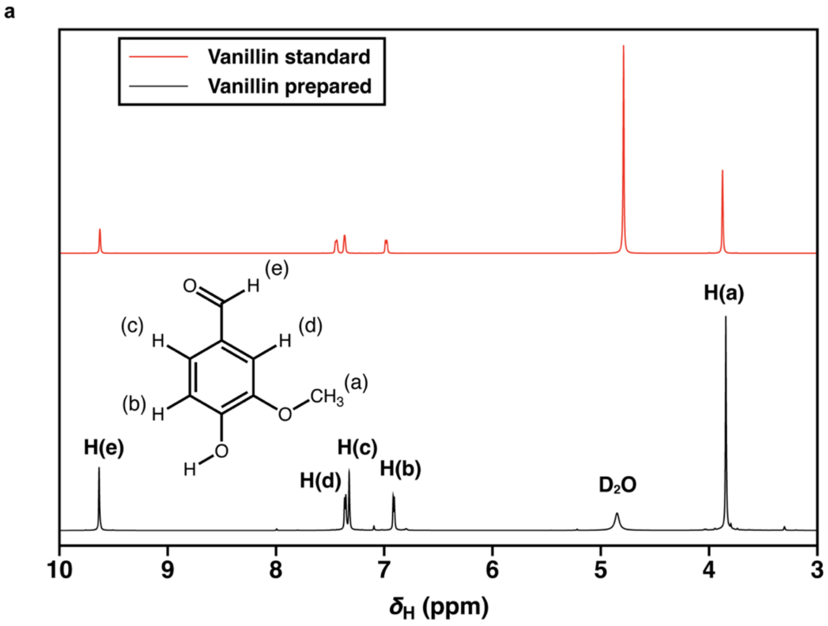

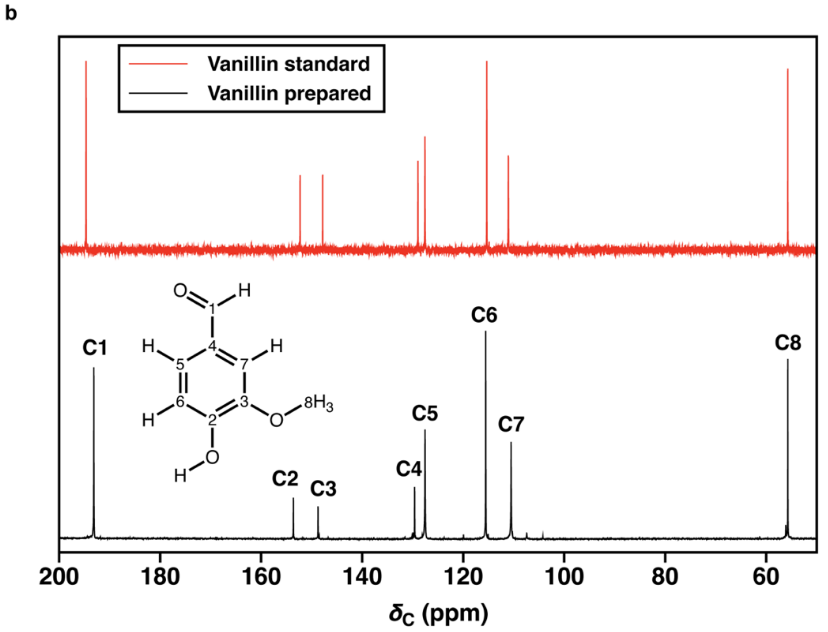

Fig. S10. NMR spectra of vanillin standard and vanillin prepared (D_2O). (a) ^{1}H-NMR. (b) ^{13}C-NMR.

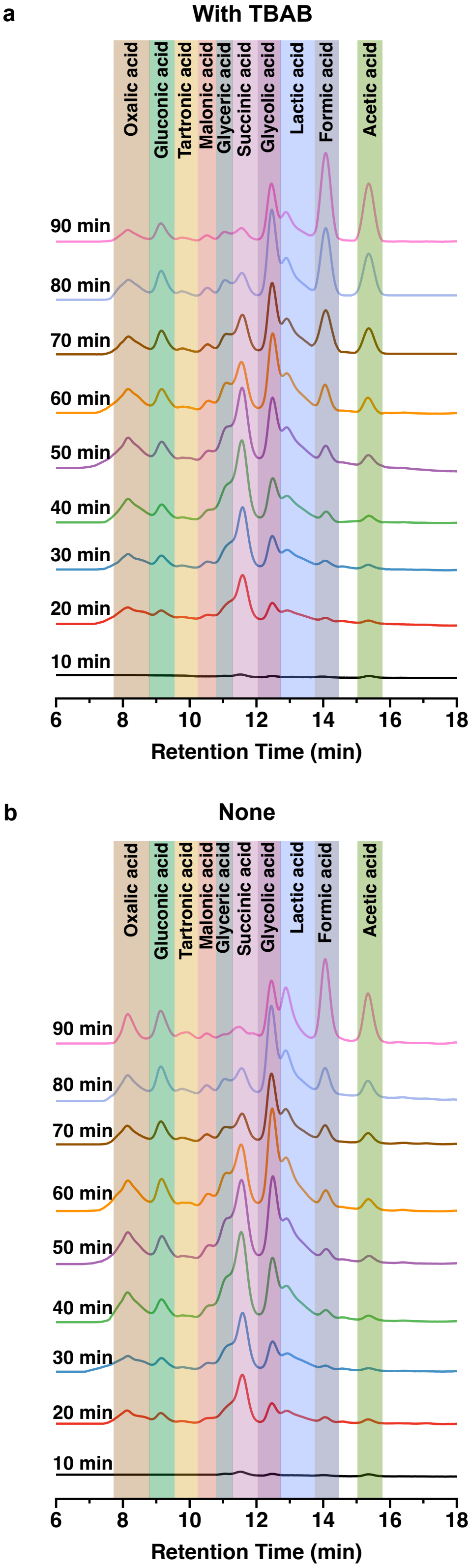

Fig. S11. HPLC spectrum of the aqueous phase product. (a) The AOD of pine wood with adding TBAB, (b) The AOD of pine wood without adding TBAB. Reaction conditions: 0.4 g pine wood, 7.5 wt% NaOH, 2.5 wt% TBAB or no addition, 160 °C, 60 min, 500 rpm, 0.4 Mpa O_2.

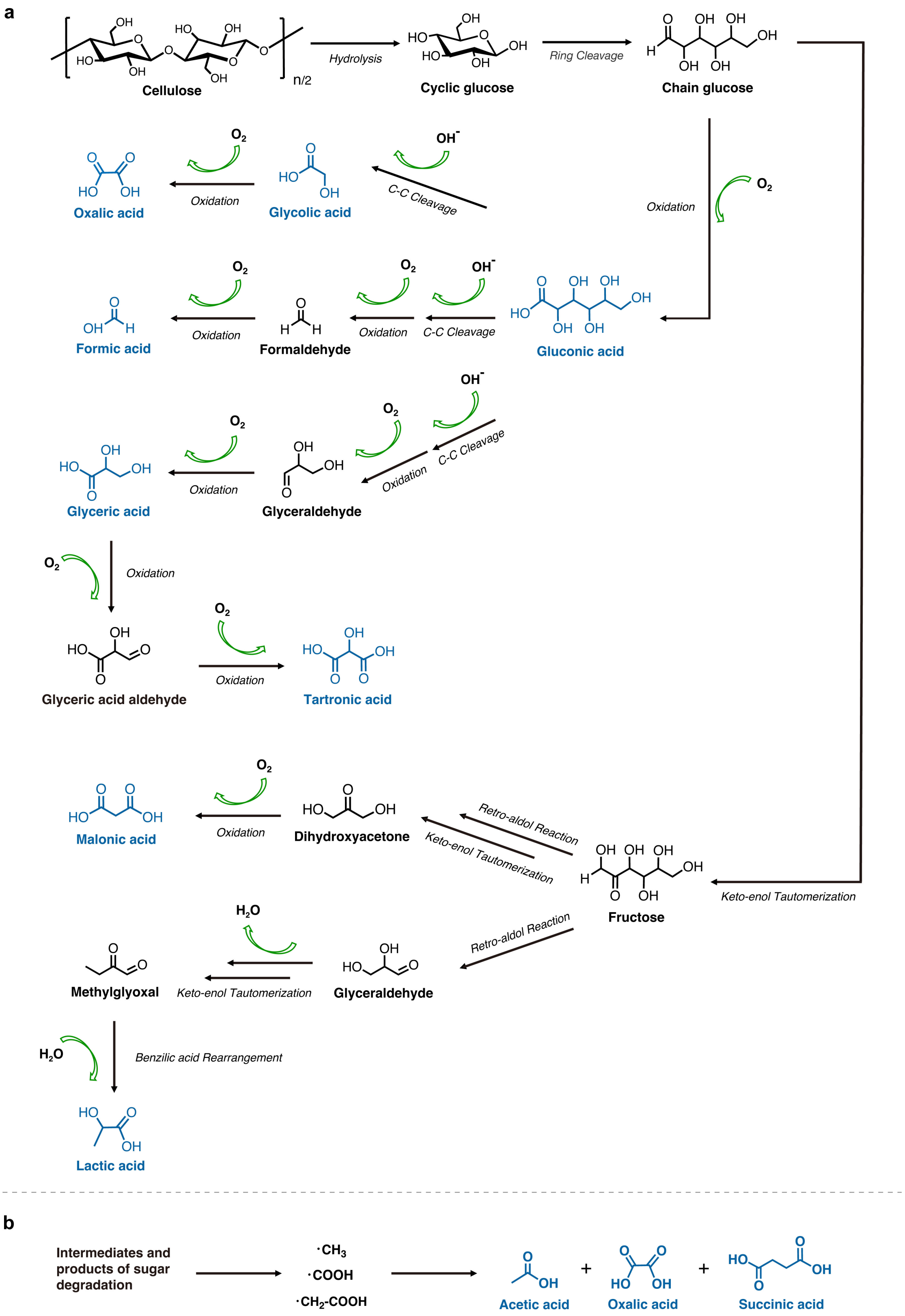

Fig. S12. The pathways of alkaline degradation of cellulose to aliphatic acids. (a) Formation of aliphatic acids via oxidation pathways, (b) Recombination of free radicals to aliphatic acids.[8]

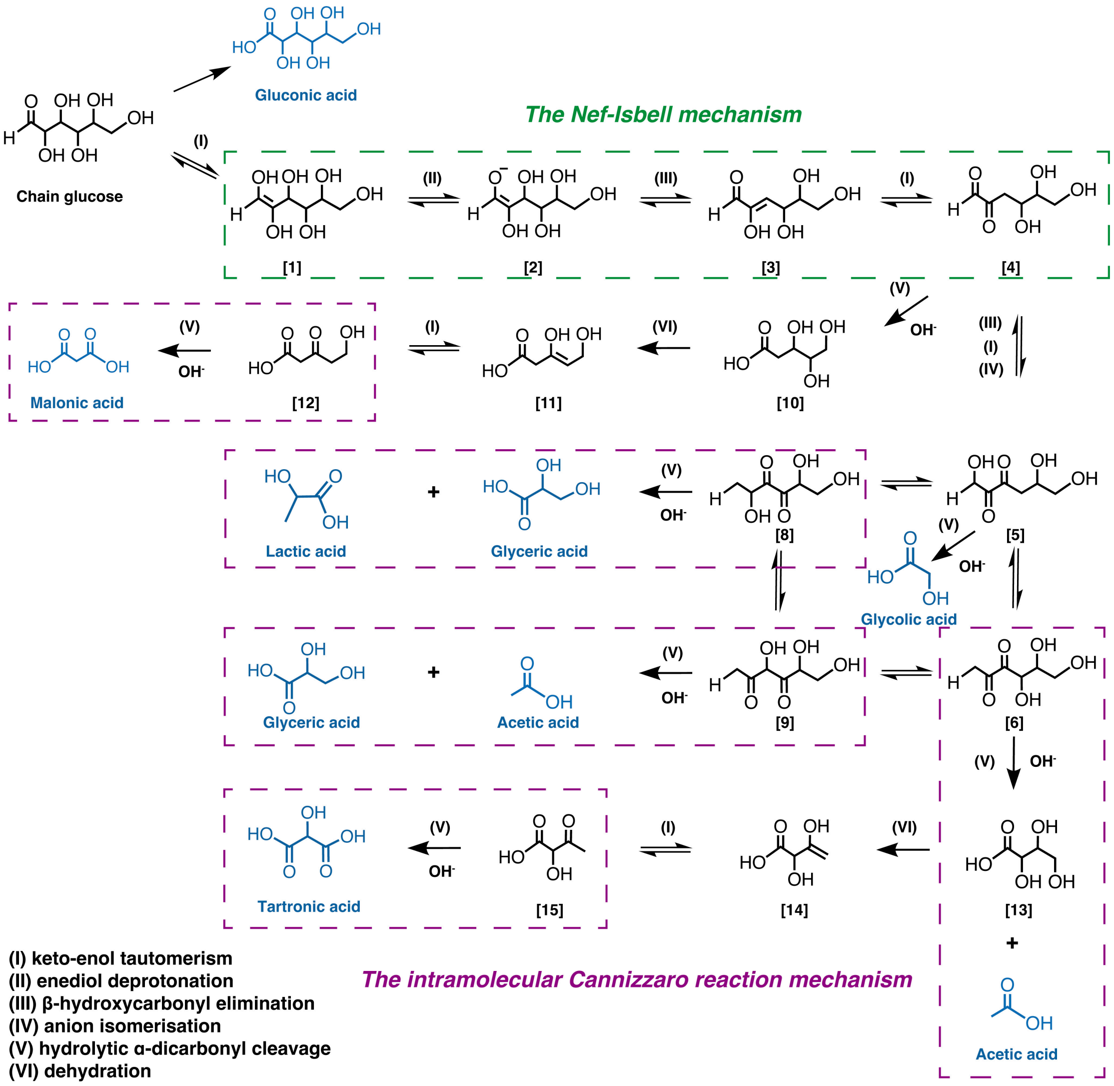

Fig. S13. The Nef-Isbell mechanism combined with the intramolecular Cannizzaro reaction mechanisms of alkaline degradation of cellulose to aliphatic acids.

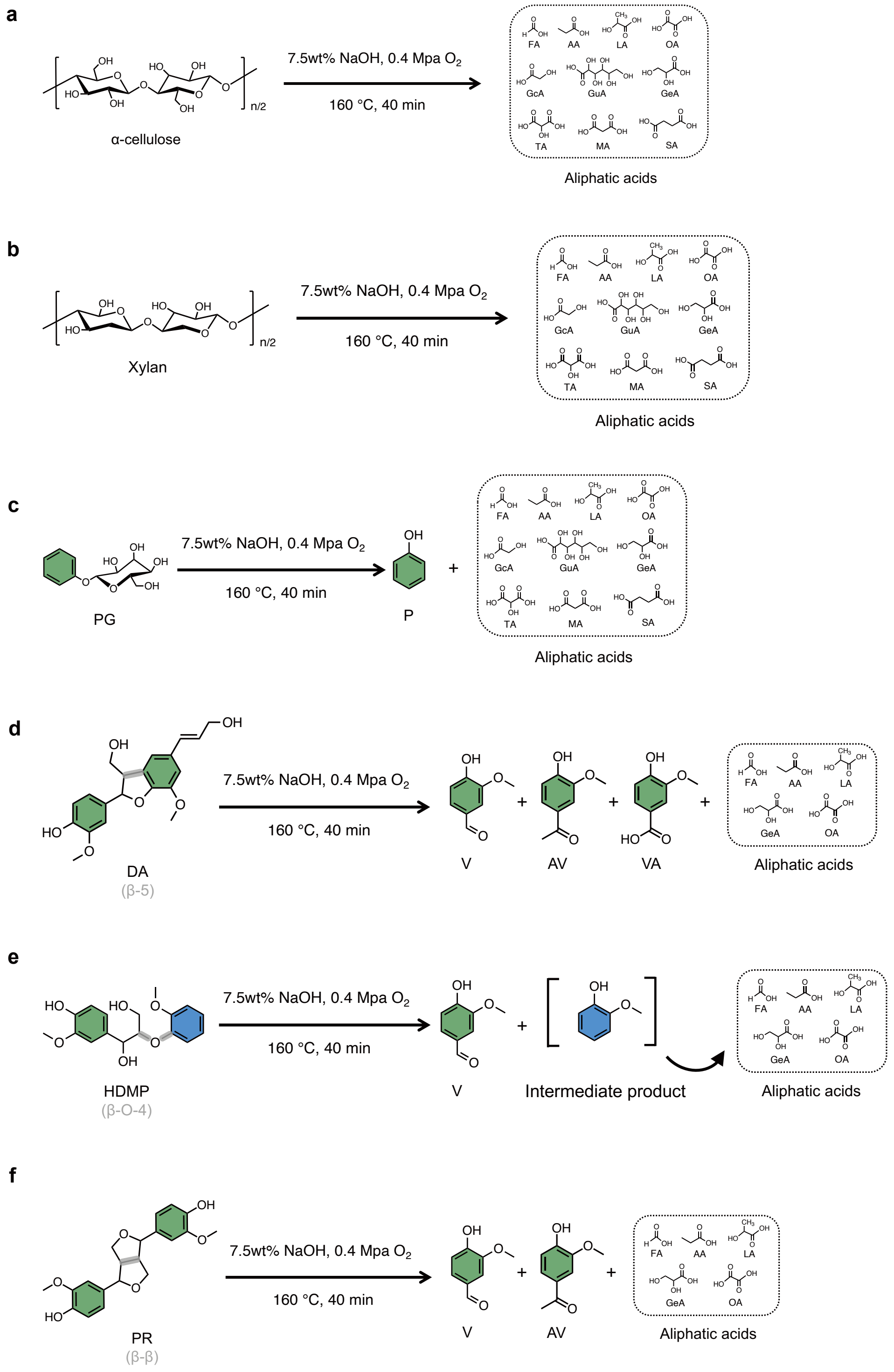

Fig. S14. Schematic diagram of the AOD reaction of model compounds**.** (a) α-cellulose, (b) xylan, (c) PG, (d) DA, (e) HDMP, (f) PR. Reaction conditions: substance (α-cellulose: 0.2 g; xylan: 0.1 g; PG: 0.1 g; DA: 0.1 g; HDMP: 0.1 g; PR: 0.1 g), 7.5 wt% NaOH, 2.5 wt% TBAB or no addition, 160 °C, 40 min, 500 rpm, 0.4 Mpa O_2.

Supplementary Note 6

The conversion of HDMP produces phenol, which is unstable under alkaline conditions and is subsequently completely converted into aliphatic acids (Fig. S14e).

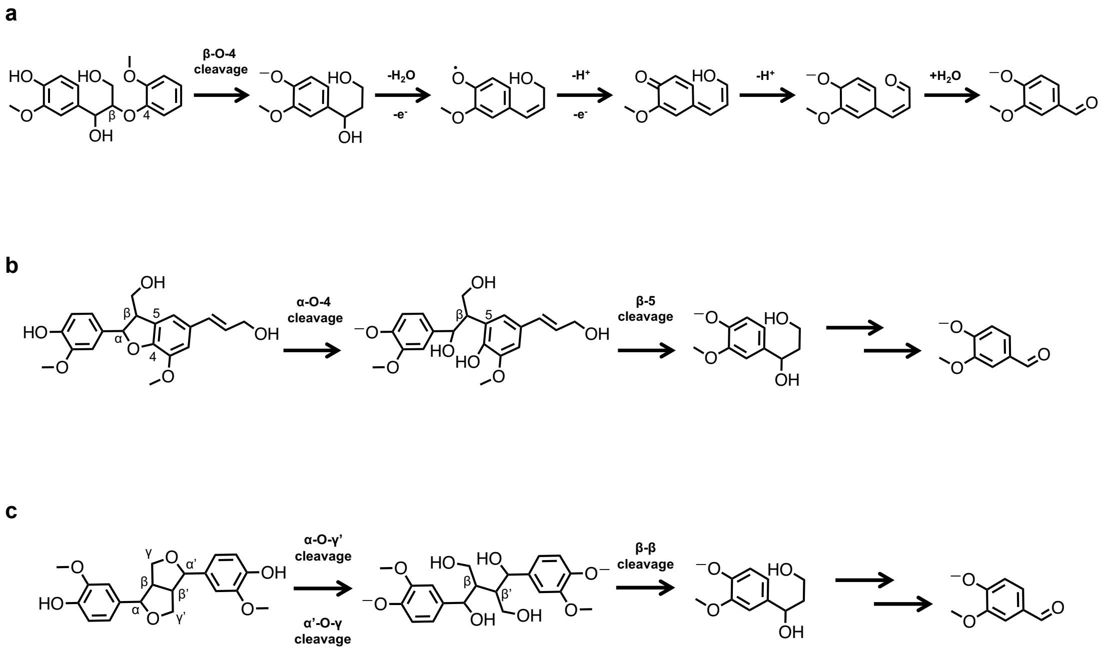

Fig. S15. Mechanistic routes for the conversion of three lignin model compounds to vanillin. (a) HDMP represents the β-O-4 bond in lignin. (b) DA represents the β-5 bond in lignin. (c) PR represents the β-β bond in lignin.

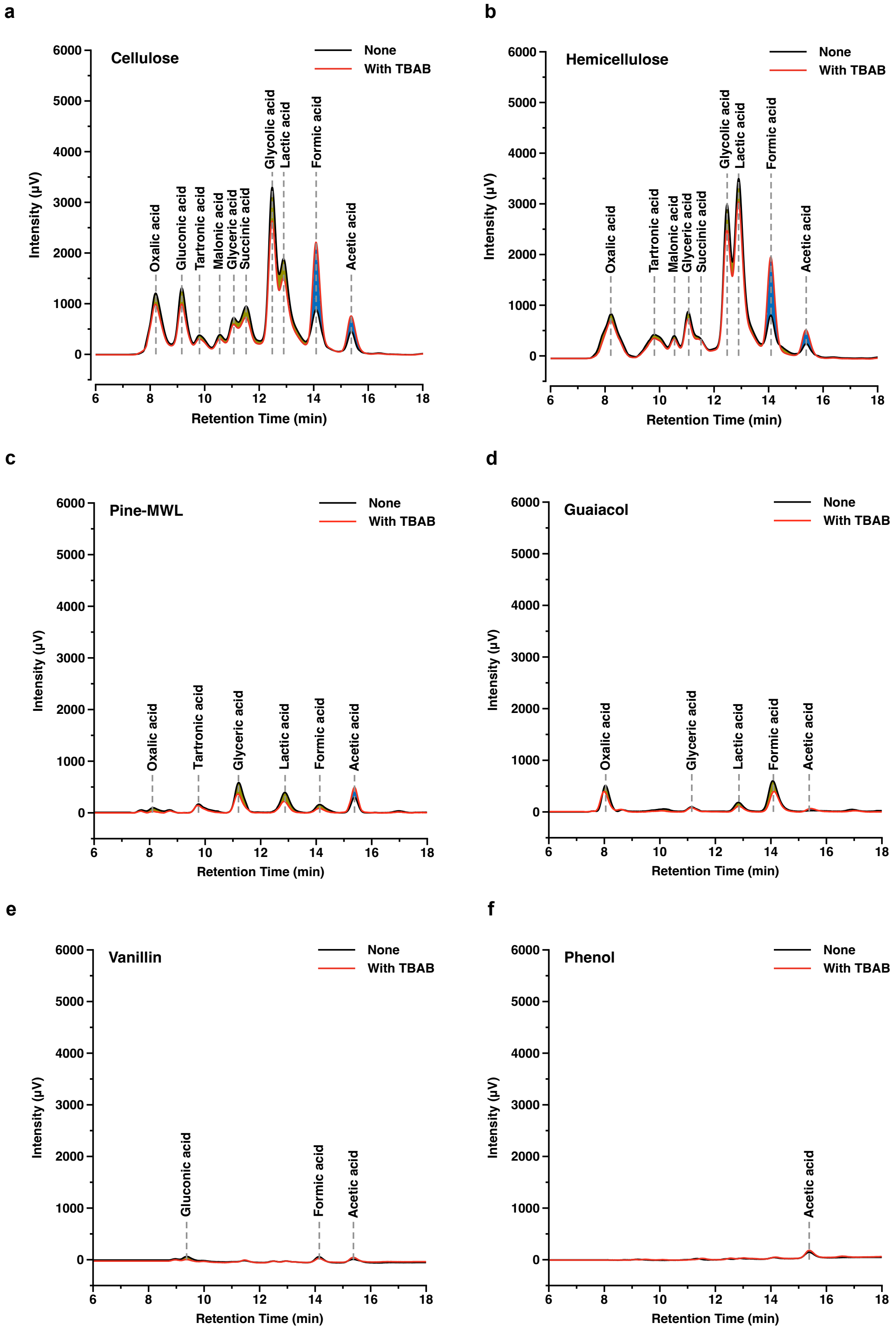

Fig. S16. HPLC spectra of the AOD reaction products of cellulose, hemicellulose, lignin, guaiacol, vanillin and phenol. (a) cellulose, (b) hemicellulose, (c) MWL, (d) guaiacol, (e) vanillin, (f) phenol. Reaction conditions: substance (cellulose: 0.2 g α-cellulose; hemicellulose: 0.1 g xylan; lignin: 0.1 g Pine-MWL; guaiacol: 0.1 g; vanillin: 0.1 g; phenol: 0.1 g), 7.5 wt% NaOH, 2.5 wt% TBAB or no addition, 160 °C, 40 min, 500 rpm, 0.4 Mpa O_2.

Supplementary Note 7

1) The areas between the peaks in the spectra are filled with colors to indicate the effect of TBAB on different substrates. Brown-green color indicates that the addition of TBAB to the reaction has an inhibitory effect on the production of aliphatic acids, and blue color indicates that the addition of TBAB to the reaction has a promoting effect on the production of aliphatic acids.

2) The comparative experiment with or without adding TBAB showed that the addition of TBAB was conducive to the production of formic acid and acetic acid in the AOD reaction of cellulose and hemicellulose. This is consistent with the results obtained using pine wood as raw material (Fig. S6c).

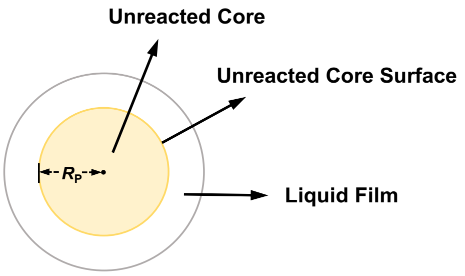

Fig. S17. The core shrinkage model of the lignin depolymerization.

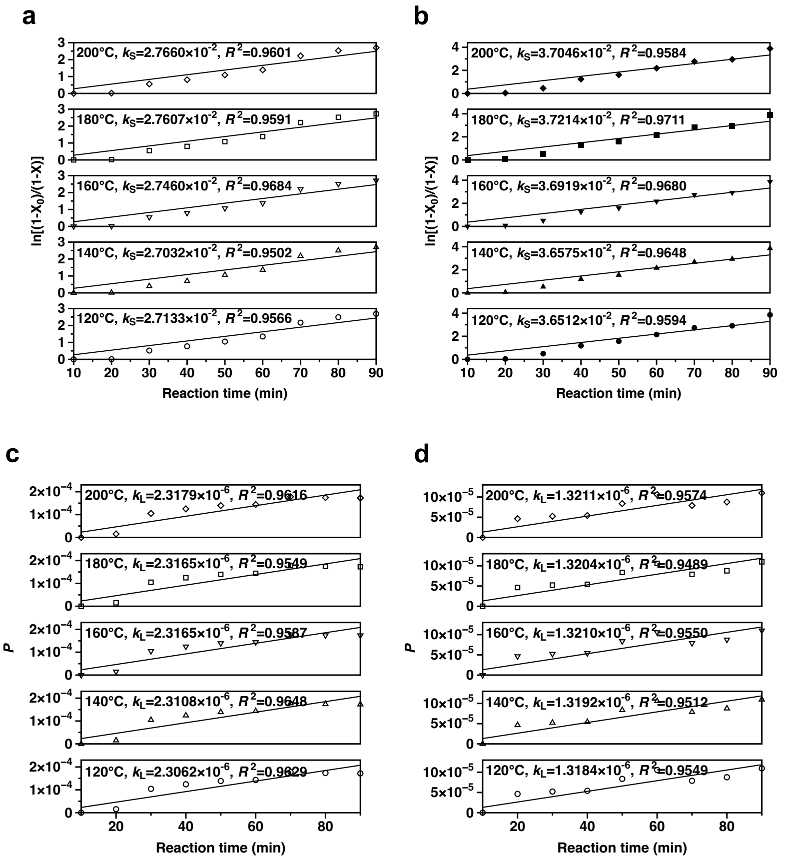

Fig. S18. Kinetic analysis of the AOD process of pine wood. The relationship between ln[(1-X_0)/(1-X)] and reaction time in a chemical reaction process: (a) Reaction without adding TBAB; (b) Reaction with TBAB. The relationship between *P* and reaction time in a liquid film mass transfer process: (c) Reaction without adding TBAB; (d) Reaction with TBAB.

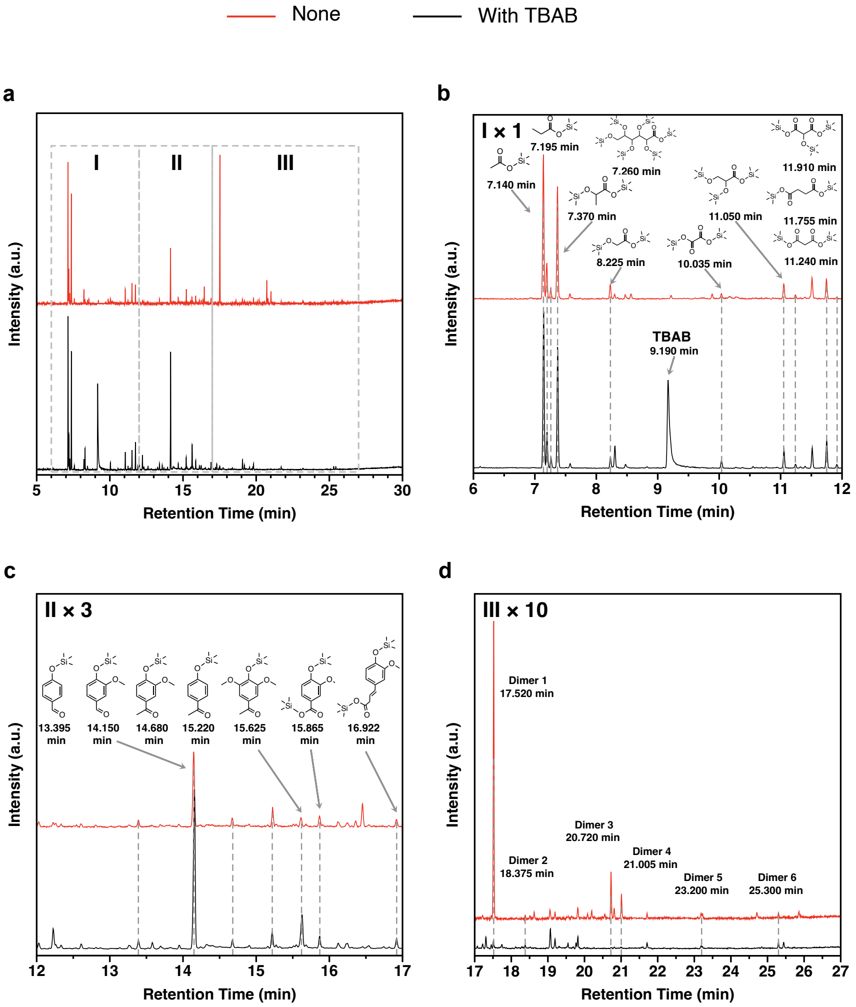

Fig. S19. GC-MS spectra of MSTFA derivatized products in the organic phase in the AOD process. Reaction conditions: 0.4 g pine wood, 7.5 wt% NaOH, 2.5 wt% TBAB or no addition, 160 °C, 40 min, 500 rpm, 0.4 Mpa O_2

Dimer 1

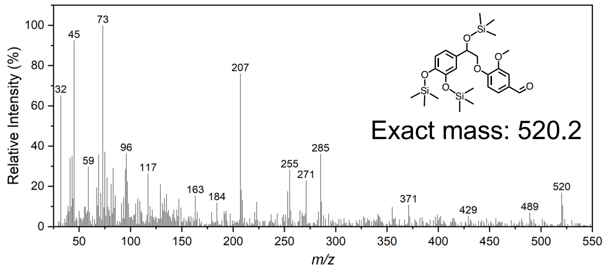

Dimer 2

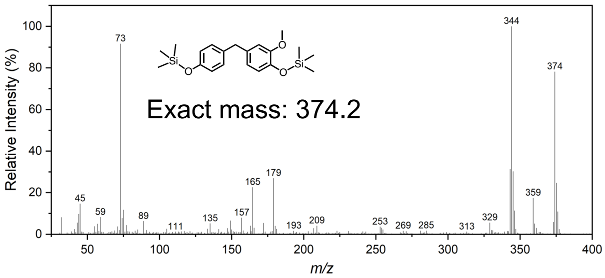

Dimer 3

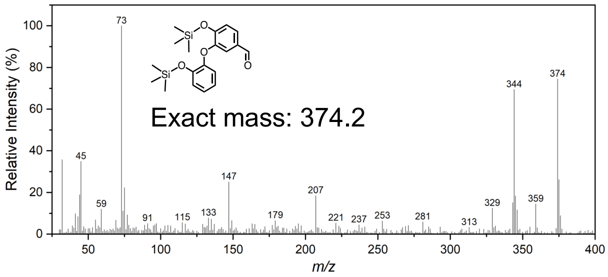

Dimer 4

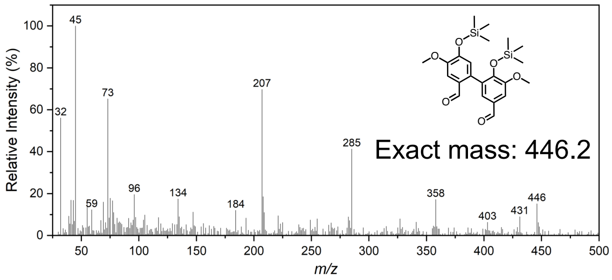

Dimer 5

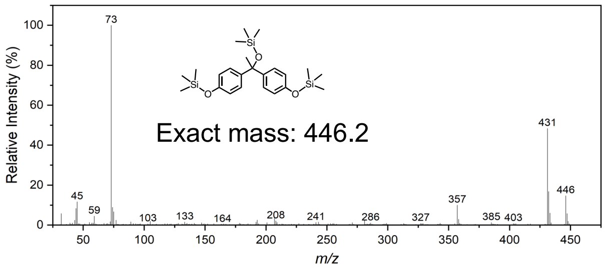

Dimer 6

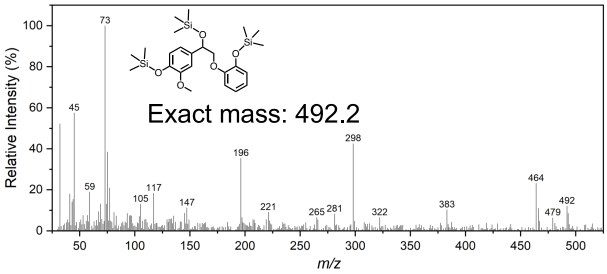

Fig. S20. The dimer structures inferred from mass spectrometry.

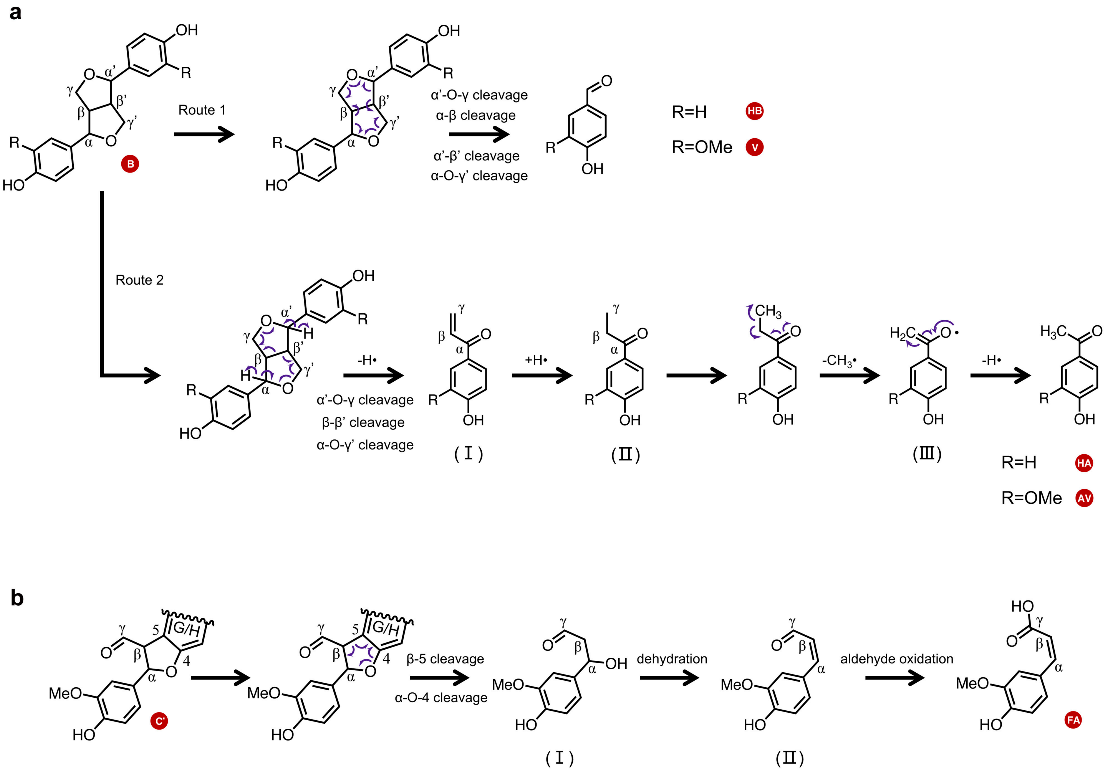

Fig. S21. The mechanism of carbon-carbon bond cleavage in structures B (a) and C' (b).

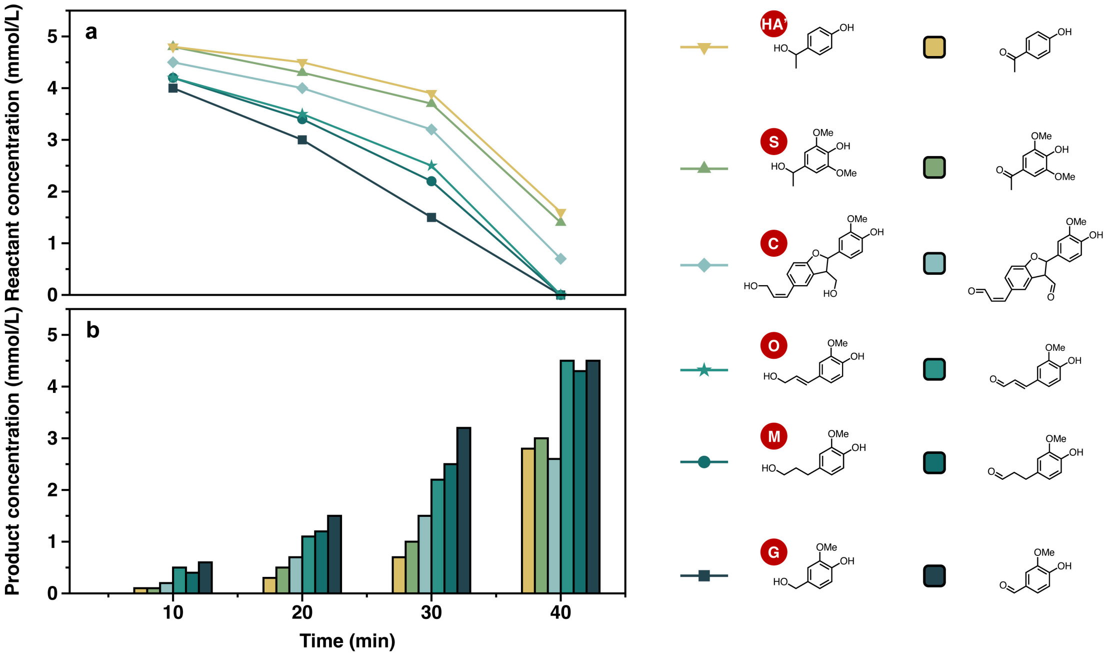

Fig. S22. Oxidation of the six lignin monomers at different times. (a) Reactant consumption curve. (b) Product generation histogram. Reaction conditions: 5 mmol L^{-1} lignin monomer, 7.5 wt% NaOH, 2.5 wt% TBAB, 160 °C, 500 rpm, 0.4 Mpa O_2, 40 min (Start timing when heating starts).

Supplementary Note 8

1) Compound C underwent pronounced ring-opening to partially yield vanillin at 40 minutes, which in turn suppressed the accumulation of hydroxyl-only oxidation products.
2) Compound M will be oxidized to dihydroconiferyl aldehyde, but the main ^{13}C-^{1}H crosslinking signals of this structure in the HSQC NMR spectra database have not been found, so the dihydroconiferyl aldehyde structure is not clear in the lignin fragments.

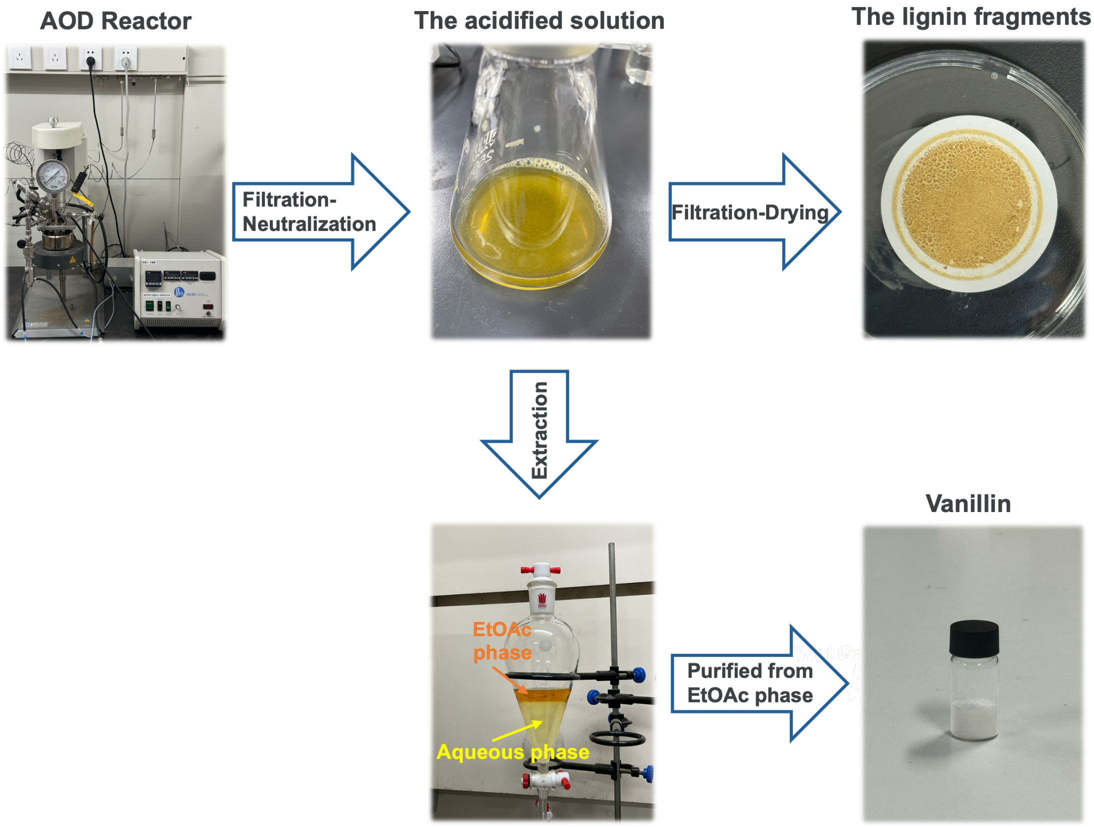

Fig. S23. Experimental operation flow chart.

Supplementary Note 9

1) In the neutralization operation, concentrated hydrochloric acid is used to acidify the liquid after the AOD reaction to a pH of 5.0.

2) The drying operation is to dry the filtered lignin fragments overnight at 60 °C.

3) The extraction operation requires the use of ethyl acetate (10 × 10 ml) to extract the aqueous phase liquid after the AOD reaction multiple times until the aqueous phase is colorless.

4) Preparative liquid chromatography was used to separate and purify the vanillin product.

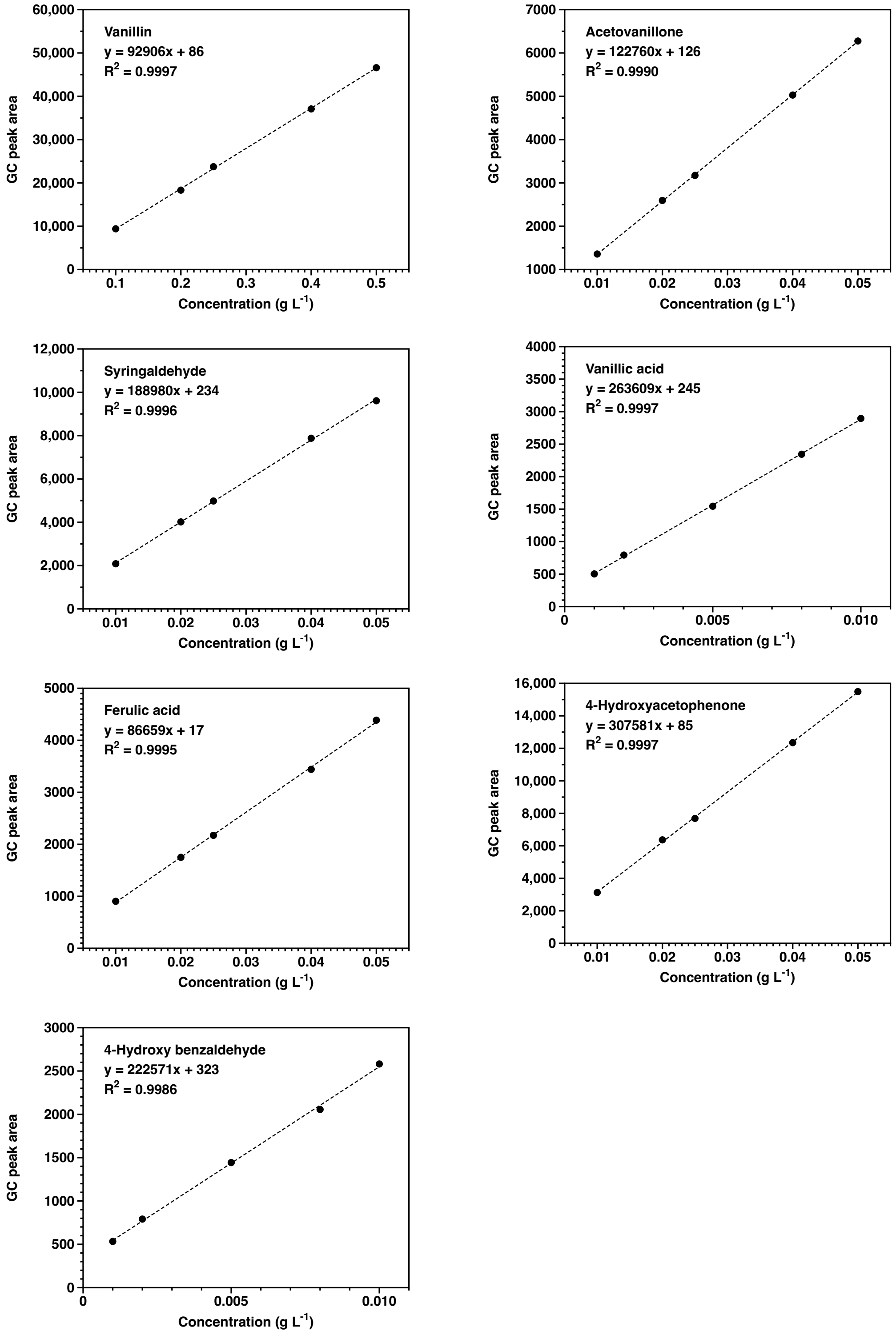

Fig. S24. GC calibration curves for lignin monomers and gases.

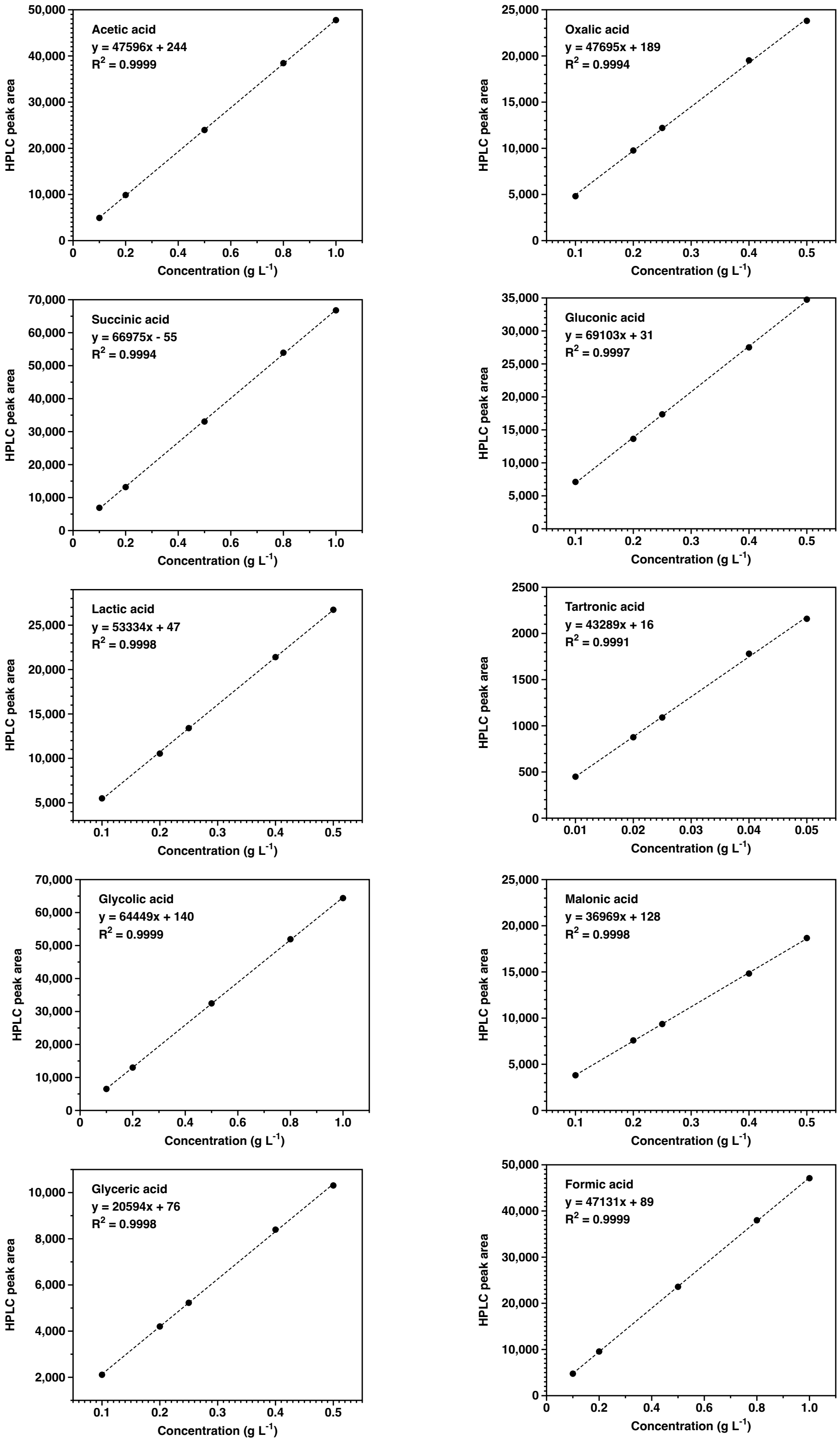

Fig. S25. HPLC refractive index detector calibration curves for aliphatic acids.

Table S1. Compositional analysis of various lignocellulosic biomass.

Samples	Lignin (wt%)	Cellulose (wt%)	Hemicellulose (wt%)	Extraction (wt%)	Total (wt%)
Pine	28.8	39.8	20.6	5.5	94.7
Poplar	23.4	49.2	17.0	4.9	94.5
Corn stover	17.5	48.1	23.5	2.7	91.8

Table S2. Lignin monomers yield, vanillin selectivity, SR, lignin fragments yield, M_w, and delignification obtained by AOD of different lignocellulosic biomass. Reaction conditions: 0.4 g biomass, 7.5 wt% NaOH, 160 °C, 1 h, 500 rpm, 1.0 Mpa O_2

Samples	Lignin monomers yield (wt%)	Vanillin sel. (%)	SR (wt%)	Lignin fragments yield (wt%)	M_w-AOD oil (g mol^{-1})	Delignification (%)
Pine	28.7	78.0	5.1	10.9	492	100
Poplar	22.5	18.4	8.5	14.2	340	100
Corn stover	8.1	23.7	2.4	18.6	253	100

Table S3. Lignin monomers yield, vanillin selectivity, SR, lignin fragments yield, M_w, and delignification obtained by AOD of pine wood with different PTC. Tabulated data from Fig. 1d. Reaction conditions: 0.4 g pine wood, 7.5 wt% NaOH, 2.5 wt% PTC, 160 °C, 40 min, 500 rpm, 0.4 Mpa O_2

PTC	Lignin monomers yield (wt%)	Vanillin sel. (%)	SR (wt%)	Lignin fragments yield (wt%)	M_w-AOD oil (g mol^{-1})	Delignification (%)
None[a]	28.7	78.0	5.1	10.9	492	100
TBAB	39.8	81.4	3.5	6.2	209	100
ACh	27.1	87.1	4.1	11.9	428	100
TBAH	22.6	84.5	3.1	23.5	282	100
α-CD	22.8	89.5	3.7	17.4	401	100
TMG	30.7	85.7	4.4	8.1	337	100

[a] The optimal yield of vanillin without PTC was obtained under the reaction conditions of 160 °C and 1.0 MPa O_2 for 1 hour, which is similar to the results of previous study.

Table S4. Phenolic monomers yield of organic phase product obtained from AOD of pine wood with TBAB at different reaction times. Tabulated data from Fig. S3a.

Reaction time (min)	Phenolic monomers yield (wt%)							Total (%)
	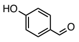	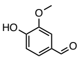	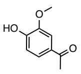	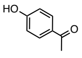	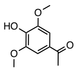	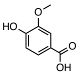	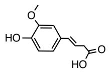	
10	n.d.	0.6	n.d.	n.d.	n.d.	n.d.	n.d.	0.6
20	n.d.	0.9	n.d.	n.d.	n.d.	n.d.	n.d.	0.9
30	0.1	6.6	0.5	0.3	0.1	0.2	0.5	8.3
40	0.2	18.2	1.5	1.0	0.5	0.5	0.7	22.6
50	0.3	25.6	2.2	1.4	0.8	0.7	0.9	31.9
60	0.4	28.5	2.8	1.3	1.0	0.6	1.3	35.9
70	0.4	32.4	2.9	1.0	1.3	0.5	1.3	39.8
80	0.5	28.0	2.7	0.4	1.3	0.3	0.5	33.7
90	0.5	27.7	2.9	0.6	1.2	0.4	0.5	33.8

Table S5. Phenolic monomers yield of organic phase product obtained from AOD of pine wood without adding TBAB at different reaction times. Tabulated data from Fig. S3b.

Reaction time (min)	Phenolic monomers yield (wt%)							Total (%)
	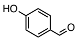	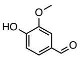	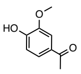	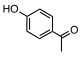	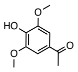	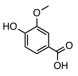	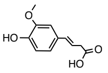	
10	n.d.	0.6	n.d.	n.d.	n.d.	n.d.	n.d.	0.6
20	n.d.	1.5	n.d.	n.d.	n.d.	0.1	n.d.	1.6
30	0.1	9.3	0.5	0.3	0.1	0.1	1.3	11.7
40	0.2	17.9	2.0	0.1	0.8	0.1	0.1	21.2
50	0.3	18.6	2.0	0.1	0.6	0.1	0.1	21.8
60	0.4	19.5	2.0	0.9	0.4	0.4	5.1	28.7
70	0.5	21.6	2.5	1.4	0.6	0.4	0.7	27.7
80	0.5	22.1	2.8	1.3	0.6	0.5	0.9	28.7
90	0.6	22.0	2.8	1.2	1.2	0.3	0.6	28.7

Table S6. The semi-quantitative analysis methods of the HSQC NMR spectra for the correlation peaks. ***I*** is the integration value of corresponding signal in spectra.

Aromatic moiety	Calculation
Total aromatic content (100 C_9 units)	$0.5[I(S_{2,6}) + I(S'_{2,6}) + I(H_{2,6}) + I(G_2) + I(G_6)]$
β-O-4	$[I(A_\gamma) + I(A'_\gamma) + I(A''_\alpha)]$ / 100 C_9
β-β	$[I(B_\beta)]$ / 100 C_9
β-5	$[I(C_\alpha)]$ / 100 C_9
β-1	$[I(E_\beta)]$ / 100 C_9
5-5	$[I(F_{\alpha,\beta}) + I(G''_6) + I(G'''_6)]$ / 100 C_9
Dihydrocinnamyl alcohol	$[I(M_\gamma)]$ / 100 C_9
Cinnamyl aldehyde	$[I(L_\gamma)]$ / 100 C_9
Acetyl	$[I(N_\beta) + I(P_\alpha)]$ / 100 C_9
H	$0.5[I(H_{2,6})]$ / 100 C_9
Oxidized H	$0.5[I(H'_{3,5})]$ / 100 C_9
G	$[I(G_2)]$ / 100 C_9
Oxidized G	$[I(G'_2)]$ / 100 C_9
S	$0.5[I(S_{2,6})]$ / 100 C_9
Oxidized S	$0.5[I(S'_{2,6})]$ / 100 C_9

Table S7. Semi-quantitative analysis of interlinkages and aromatic moieties of the Pine-MWL and AOD oil obtained from the AOD of pine wood.

Aromatic moiety	Samples		
	Pine-MWL	AOD oil	
		None	With TBAB
Interunit linkages (per 100 C_9 units)			
β-O-4 (A + A' + A'')	9.1	n.d.	n.d.
β-β resinol (B)	3.9	n.d.	n.d.
β-5 phenylcoumaran (C)	1.5	n.d.	n.d.
β-1 (E)	1.0	n.d.	n.d.
5-5 dibenzodioxocin (F)	0.2	n.d.	n.d.
5-5 dehydrodivanillin and ethyl ketone (G'' + G''')	n.d.	4.6	1.2
Total	15.7	4.6	1.2
Lignin end-groups (per 100 C_9 units)			
Dihydrocinnamyl alcohol (M)	0.8	0.7	0.2
Cinnamyl aldehyde (L)	n.d.	0.5	0.4
Acetyl (N + P)	n.d.	0.4	0.3
Lignin aromatic units (%)			
H	2.7	n.d.	n.d.
Oxidized H (H')	n.d.	4.0	3.3
G	96.1	4.3	1.7
Oxidized G (G')	n.d.	90.4	91.9
S	1.2	n.d.	n.d.
Oxidized S (S')	n.d.	1.3	3.1

Table S8. Recent works on the depolymerization of biomass to vanillin.

Feedstock	Catalyst	Reaction conditions	Vanillin yield (wt%)	Lignin monomers yield (wt%)	Reference
Pine	**NaOH / TBAB**	**160** °C**, 0.4 Mpa O_2, 40 min**	**32.4**	**39.8**	**This work**
Pine	NaOH	160 °C, 1.0 Mpa O_2, 60 min	21.1	29.0	21
Pine	NaOH / $LaMn_{0.8}Cu_{0.2}O_3$	175 °C, 5 bar O_2 + 15 bar He, 10 min	17.5	22.0	22
Pine	NaOH / CuO	160 °C, 1.0 Mpa O_2, 60 min	25.9	33.8	23
Cedar	Bu_4NOH	120 °C, 1 bar Air, 43 hours	15.4	22.5	24
Pine	NaOH / nitrobenzene	190 °C, 90 min	16.7	18.3	25
Birch	NaOH / $Cu(OH)_2$	170 °C, 0.3 Mpa O_2, 20 min	13.0	34.4	26
Cedar	NaOH / Bu_4NOH	120 °C, 1 bar O_2, 4 hours	23.2	24.4[a]	27

[a]The authors only provided vanillin and vanillic acid yield data, and the total lignin monomers yield was the sum of the two monomers.

Table S9. Semi-quantitative analysis of substructures in lignin fragments at different times. Tabulated data from Fig. 3b. Results are presented as percentages.

Time (min)	Lignin substructures (per 100 C_9 units, %)											
	B	C’	E’	F	G	G’	G’’	J	N	Q	S’	W
10	12	8	3	10	19	26	0	0	0	0	5	17
20	8	9	3	9	12	38	0	0	0	2	5	15
30	5	0	0	9	0	67	0	0	6	8	5	0
40	2	0	0	4	0	73	0	0	8	12	2	0
50	0	0	0	0	0	39	5	42	15	0	0	0
60	0	0	0	0	0	31	7	47	16	0	0	0
70	0	0	0	0	0	19	17	47	17	0	0	0

Table S10 Assignments of main ^{13}C-^{1}H crosslinking signals in the HSQC NMR spectra[9-14].

Labels	δ_C/δ_H (ppm)	Assignments
CH_3	15.1/0.9	CH_3 in aliphatic acid chain
CH_3	16.4/1.3	CH_3 in aliphatic chain
CH_2	19.7/2.2	CH_2 in aliphatic chain ($-CH_2-CH_2-CH_3$)
CH_2	22.5/1.6	CH_2 in aliphatic chain ($-CH_2-CH_2-CH_3$)
CH_2	25.2/1.3	CH_2 in aliphatic acid chain ($-CH_2-CH_2-CH_3$)
$C_\alpha H_3$	25.2-29.4/2.3-2.6	$C_\alpha H_3$ in oxidized G units (G’ and G’”) and oxidized H units (H’ and H’”)
M_α	31.07/2.51	C_α-H_α in dihydrocinnamyl alcohol (M)
CH_2	33.1/2.2	CH_2 in aliphatic acid chain ($-CH_2-CH_2-CH_3$)
M_β	37.11/1.66	C_β-H_β in dihydrocinnamyl alcohol (M)
B’$_\beta$	50/2.6	C_β-H_β in β-β (tetrahydrofuran) (B’)
C_β	52.77/3.45	C_β-H_β in phenylcoumaran (C)
C’$_\beta$	53.21/3.50	C_β-H_β in oxidized phenylcoumaran (C’)
B_β	53.45/3.29	C_β-H_β in β-β (resinol) (B)
P_β	53.57/3.61	C_β-H_β in substructure P
Ar-OMe	55.64/3.79	C-H in methoxyl in the guaiacyl units (G)
K_β	56.58/2.87	C_β-H_β in β-1 substructures (K)
$S1_\gamma$	57.91/3.92	C_γ-H_γ in di-enol substructure (S1)
TBAB	58.21/3.24	C-H in aliphatic chain in TBAB
D_β	59.54/2.77	C_β-H_β in spirodienones (D)
I_γ	61.26/4.09	C_γ-H_γ in cinnamyl alcohol (I)
W_γ	61.7/4.0	C_γ-H_γ in phenylglycerol substructure (W)
A_γ	62/3.4 and 3.8	C_γ-H_γ in β-O-4 substructures (A)
O_γ	62.50/4.2	C_γ-H_γ in Coniferyl alcohol (O)
A’$_\gamma$	62.62/4.2-4.7	C_γ-H_γ in γ-acetylated β-O-4 substructures (A’)
M_γ	62.68/3.52	C_γ-H_γ in dihydrocinnamyl alcohol (M)
N_γ	63.9/3.5	C_γ-H_γ in dihydrocinnamyl (N)
I’$_\gamma$	64.0/4.79	C_γ-H_γ in acetylated cinnamyl alcohol (I’)
$R1_\gamma$	64.87/4.22	C_γ-H_γ in propenol substructure (R1)
C_γ	66.14/3.68	C_γ-H_γ in phenylcoumaran (C)
L_α	66.84/4.12	C_α-H_α in cinnamyl aldehyde end-groups (L)
$R2_\gamma$	70.63/4.16	C_γ-H_γ in propenol substructure (R2)
B_γ	71.02/3.84 and 4.2	C_γ-H_γ in β-β (resinol) (B)
$A_{\alpha(G)}$	71.07/4.74	C_α-H_α in β-O-4 substructures linked to a G unit (A)
W_α	71.5/5.15	C_α-H_α in phenylglycerol substructure (W)
$A_{\alpha(S)}$	71.76/4.87	C_α-H_α in β-O-4 substructures linked to a S unit (A)
K_α	74.21/4.96	C_α-H_α in β-1 substructures (K)
W_β	75.9/3.66	C_β-H_β in phenylglycerol substructure (W)
D’$_\beta$	79.34/4.12	C_β’-H_β’ in spirodienones substructures (D)
E_α	79.5/5.65	C_α-H_α in α,β-diaryl ethers (E)
A’$_{\beta(G)}$	80.49/4.51	C_β-H_β in acetylated β-O-4 linked to G (A’)

Labels	δ_C/δ_H (ppm)	Assignments
D_α	81.0/5.11	C_α-H_α in spirodienones substructures (D)
E'_α	82.32/5.73	C_α-H_α in oxidized α,β-diaryl ethers (E’)
B'_α	83.02/5.01	C_α-H_α in β-β (tetrahydrofuran) (B’)
A''_α	83.01/5.25	C_β-H_β in (C_α=O) β-O-4 substructures (A’’)
F_α	83.13/4.83	C_α-H_α in 5-5 (dibenzodioxocin) substructures (F)
$A_{\beta(G/H)}$	83.47/4.39	C_β-H_β in β-O-4 substructures linked to G/H (A)
B_β	84.79/4.63	C_β-H_β in β-β (resinol) (B)
F_β	85.31/3.86	C_β-H_β in 5-5 (dibenzodioxocin) substructures (F)
D'_α	85.94/4.38	C_α'-H_α' in spirodienone substructures (D)
$A_{\beta(S)}$	86.0/4.12	C_β-H_β in β-O-4 substructures linked to S (A, Erythro)
$A_{\beta(S)}$	86.64/3.97	C_β-H_β in β-O-4 substructures linked to S (A, Thero)
T_8	93.83/6.58	C_8-C_8 in tricin (T)
C_α	98.12/5.62	C_α-H_α in phenylcoumaran (C)
T_6	98.68/6.24	C_6-C_6 in tricin (T)
$S_{2,6}$	102.6/6.75	C_2-H_2 in syringyl units (S)
$T_{2,6}$	103.67/7.32	$C_{2,6}$-$C_{2,6}$ in tricin (T)
T_3	104.51/7.05	C_3-C_3 in tricin (T)
$L_{2,6(S)}$	105.95/7.05	$C_{2,6}$-$H_{2,6}$ in sinapaldehyde end-groups (L)
$S'_{2,6}$	106.32/7.16	C_2-H_2 in oxidized syringyl units (S’)
C'_α	107.05/5.91	C_α-H_α in oxidized phenylcoumaran (C’)
G'_2	110.57/7.37	C_2-H_2 in C_α=O oxidized guaiacyl units (G’)
G_2	110.81/6.98	C_2-H_2 in guaiacyl units (G)
G''_2	111.08/7.43	C_2-H_2 in dehydrodivanillin substructures (G’’)
$J_{3,5}$	111.32/6.88	$C_{3,5}$-$H_{3,5}$ in p-coumarate (J)
Q_2	113.77/7.62	C_2-H_2 in ferulate (Q)
$G_5/H_{3,5}$	114.85/6.76	C_5-H_5 in guaiacyl units (G) and $C_{3,5}$-$H_{3,5}$ in H units(H)
$H'_{3,5}$	114.97/6.87	$C_{3,5}$-$H_{3,5}$ in C_α=O oxidized H units (H’)
G'_5	115.44/7.02	C_5-H_5 in C_α=O oxidized guaiacyl units (G’)
G_6	118.67/6.78	C_6-H_6 in guaiacyl units (G)
G''_6/G'''_6	121.5-129.8/7.8-8.1	C_6-C_6 in dehydrodivanillin (G’’) and dehydrovanillin ethyl ketone substructures(G’’’)
G'_6	122.7-128.6/6.8-7.6	C_6-C_6 in C_α=O oxidized guaiacyl units (G’)
$S1_\alpha$	125.05/6.71	C_α-H_α in di-enol substructure (S1)
Q_6	125.85/7.43	C_6-H_6 in ferulate (Q)
$R2_\alpha$	125.66/7.95	C_α-H_α in propenol substructure (R2)
L_β	126.08/6.76	C_β-H_β in cinnamyl aldehyde end-groups (L)
$H_{2,6}$	127.42/7.6	$C_{2,6}$-$H_{2,6}$ in H units (H)
$R1_\alpha$	128.09/7.69	C_α-H_α in propenol substructure (R1)
I_α	128.26/6.44	C_α-H_α in cinnamyl alcohol (I)
I_β	128.26/6.25	C_β-H_β in cinnamyl alcohol (I)
$J_{2,6}$	129.95/7.47	$C_{2,6}$-$H_{2,6}$ in p-coumarate (J)
$H'_{2,6}/H''_{2,6}/H'''_{2,6}$	131.86/7.76	$C_{2,6}$-$H_{2,6}$ in C_α=O oxidized H units (H’, H’’, H’’’)

Table S11. The aliphatic acids yield of aqueous phase product obtained from the AOD of different time with adding TBAB. Tabulated data from Fig. S6c.

Reaction time (min)	Aliphatic acids yield (wt%)										Total yield (wt%)
	OA	GuA	TA	MA	GeA	ScA	GcA	LA	FA	AA	
10	n.d.	n.d.	n.d.	n.d.	0.50	0.25	0.25	n.d.	n.d.	0.50	1.49
20	1.74	1.74	n.d.	1.49	1.49	12.42	6.71	1.24	1.99	1.24	30.05
30	1.99	2.24	n.d.	2.24	2.24	15.65	8.94	2.48	3.48	2.24	41.47
40	3.73	2.48	n.d.	3.23	3.23	22.60	10.93	2.73	5.46	2.98	57.37
50	4.47	3.73	0.25	3.73	3.73	20.36	16.89	3.48	7.20	4.47	68.29
60	5.22	4.22	0.25	3.97	3.97	15.15	20.61	3.73	9.19	6.21	72.52
70	4.20	4.97	0.50	4.15	3.48	11.18	22.10	4.24	11.92	12.17	78.91
80	4.22	5.71	0.75	4.97	3.48	7.45	17.88	4.97	17.38	15.89	82.70
90	3.23	3.97	0.50	3.48	1.99	2.48	15.15	5.46	28.56	17.63	82.45

Table S12. The aliphatic acids yield of aqueous phase product obtained from the AOD of different time without adding TBAB. Tabulated data from Fig. S6c.

Reaction time (min)	Aliphatic acids yield (wt%)										Total yield (wt%)
	OA	GuA	TA	MA	GeA	ScA	GcA	LA	FA	AA	
10	n.d.	n.d.	n.d.	n.d.	0.57	0.28	0.28	n.d.	n.d.	0.57	1.70
20	1.42	1.98	n.d.	1.42	1.13	15.87	7.08	1.42	1.70	1.13	33.15
30	1.42	1.98	n.d.	1.98	1.98	18.14	8.22	2.27	0.85	0.57	37.40
40	5.10	4.53	0.28	3.12	3.12	24.65	17.57	3.12	2.27	1.42	65.17
50	5.67	5.67	0.57	3.68	3.40	21.82	22.67	3.68	3.40	2.27	72.82
60	6.23	6.80	0.57	3.97	3.97	18.70	29.19	4.53	4.82	4.25	83.02
70	4.53	5.95	0.85	4.25	3.40	14.40	38.74	4.82	5.10	4.53	86.58
80	4.53	7.08	1.42	4.53	3.12	10.43	37.25	5.38	8.50	5.10	87.35
90	4.25	7.93	1.98	2.83	1.42	2.55	16.15	11.05	26.35	14.89	89.42

Table S13. The aliphatic acids yield of aqueous phase product obtained from the AOD of different substances with adding TBAB. Tabulated data from Fig. S16.

Substance	Conversion (%)	Aliphatic acids yield (wt%)										Total yield (wt%)
		OA	GuA	TA	MA	GeA	ScA	GcA	LA	FA	AA	
Cellulose	97.1	2.5	5.3	0.4	2.5	1.1	11.6	17.9	1.8	7.7	6.0	56.4
Hemicellulose	>99.9	5.2	n.d.	3.0	6.2	5.0	6.2	31.9	7.2	13.0	9.1	86.8
Pine-MWL	>99.9	n.d.	n.d.	0.3	n.d.	1.5	n.d.	n.d.	0.5	0.2	5.0	7.5
Guaiacol	>99.9	1.8	n.d.	n.d.	n.d.	0.6	n.d.	n.d.	0.3	4.8	0.3	7.8
Vanillin	56.8	n.d.	0.1	n.d.	n.d.	n.d.	n.d.	n.d.	n.d.	0.2	0.4	0.7
Phenol	36.2	n.d.	n.d.	n.d.	n.d.	n.d.	n.d.	n.d.	n.d.	n.d.	0.8	0.8

Table S14. The aliphatic acids yield of aqueous phase product obtained from the AOD of different substances without adding TBAB. Tabulated data from Fig. S16.

Substance	Conversion (%)	Aliphatic acids yield (wt%)										Total yield (wt%)
		OA	GuA	TA	MA	GeA	ScA	GcA	LA	FA	AA	
Cellulose	93.8	3.0	6.8	0.4	2.6	1.5	16.5	23.3	3.0	3.8	3.4	64.1
Hemicellulose	>99.9	5.5	n.d.	3.1	6.2	5.5	6.2	39.0	10.9	7.0	4.7	88.1
Pine-MWL	>99.9	0.1	n.d.	0.3	n.d.	3.6	n.d.	n.d.	1.2	0.2	4.8	10.2
Guaiacol	>99.9	1.8	n.d.	n.d.	n.d.	0.6	n.d.	n.d.	0.4	6.6	0.3	9.7
Vanillin	53.4	n.d.	0.3	n.d.	n.d.	n.d.	n.d.	n.d.	n.d.	0.2	0.4	0.9
Phenol	35.5	n.d.	n.d.	n.d.	n.d.	n.d.	n.d.	n.d.	n.d.	n.d.	0.8	0.8

Table S15. The solubility, ionic radius and interfacial behavior of PTCs. Solubility data are for 25 °C unless noted. Ionic radius is approximate. Interfacial activity indicates relative surface tension effects and inclusion behavior.

PTC	Water solubility	Ionic radius & charge	Interfacial activity / surface tension behavior
TBAB	**600 g L^{-1} (20 °C)**	**Large bulky cation (~ 0.5 nm); Br^- counterion**	**Strong surfactant-like cation; dramatically lowers interfacial tension**
ACh	~100 g L^{-1}	Small cation (~ 0.25 nm); chloride	No significant surface activity; very hydrophilic (LogP ≈ -3.9)
TBAH	Fully miscible in H_2O	Same large cation as TBAB (~ 0.5 nm); OH^-	TBA^+ tends to adsorb at interface, but OH^- is strongly hydrophilic
α-CD	145 g L^{-1}	Non-ionic macrocycle (no free ion)	Water-soluble host with hydrophobic cavity; forms inclusion complexes, no ionic phase-transfer
TMG	> 600 g L^{-1}	Small zwitterion (quaternary NH^+ / COO^-)	Zwitterionic surfactant (amphoteric); limited hydrophobic character

Supplementary Note 10

1) The superior performance of TBAB as a PTC arises from its unique molecular balance of hydrophobicity and ionic character. The tetrabutylammonium cation (TBA^+) is large and strongly hydrophobic (four butyl chains), while still being highly soluble in water (~ 600 g L^{-1} at 20 °C). In solution TBAB markedly reduces the water / organic interfacial tension. Molecular simulations show that TBAB solutions have lower surface tension and enhanced adsorption of hydrophobic species at the interface compared to pure water. In fact, TBA^+ preferentially accumulates at hydrophobic interfaces over small ions, effectively concentrating the lignin fragments and O_2 at the boundary. This amphiphilic "surfactant" behavior (Table S15) accelerates transfer of phenolic intermediates out of the lignin-rich phase, leading to faster bond cleavage and higher yields of vanillin.

2) By contrast, smaller or more hydrophilic catalysts lack this effect. For example, acetylcholine chloride (ACh) is a much smaller, highly polar ion (log P ≈ -3.9) and dissolves readily in water (~ 100 g L^{-1}) but has essentially no surfactant character. It cannot concentrate aromatic fragments at the phase boundary, so it drives depolymerization less effectively.

3) Likewise, trimethylglycine (TMG) is a zwitterion that is extremely water-soluble, but its lack of long hydrophobic tails limits any interfacial activity (it functions as a mild amphoteric surfactant only). These more hydrophilic PTCs simply reside in the bulk aqueous phase and do not enhance the migration of hydrophobic lignin fragments, resulting in lower vanillin yields.

4) Tetrabutylammonium hydroxide (TBAH) shares the same bulky TBA^+ cation as TBAB (Table S15), so in principle it can also adsorb at interfaces. However, the hydroxide anion makes the medium much more strongly basic and reactive. This can promote unwanted side reactions (self-condensation of lignin fragments or over-oxidation) that compete with vanillin formation. Moreover, unlike TBAB, TBAH does not introduce a noncoordinating anion; bromide may itself participate in redox chemistry (e.g. transient HOBr formation) to further cleave lignin bonds. Overall, TBAB's combination of a large lipophilic cation and non-nucleophilic counterion yields optimal phase-transfer conditions.

5) α-Cyclodextrin (α-CD) is a special case: it is a neutral cyclic oligomer with a hydrophobic interior cavity, rather than a classical ionic PTC. It is moderately water-soluble (≈ 145 g L^{-1} at 25 °C) and binds small organic molecules via host-guest inclusion. In lignin oxidation, α-CD can modestly solubilize aromatic fragments by inclusion, but it cannot transfer ions between phases. Without ionic charge to shuttle phenolate species, it functions only as a solubilizing aid. Consequently, α-CD produces less acceleration of depolymerization than TBAB, since it does not significantly lower surface tension or carry charged lignin phenoxides to the bulk solution.

6) In summary, the molecular characteristics correlate closely with catalytic effect: TBAB has large ionic radius and hydrophobicity lead to strong interfacial activity, whereas ACh and TMG (small, polar ions) do not. The inclusion capacity of α-CD is inferior to that of ionic phase transfer. These differences explain why vanillin yields are highest with TBAB. By reducing interfacial tension and rapidly ferrying cleaved aromatic fragments into the aqueous phase, TBAB minimizes the contact time of reactive intermediates and thus suppresses their repolymerization. The result is a faster, more efficient depolymerization: TBAB both speeds up carbon-carbon and carbon-oxygen bonds cleavage steps and ensures that vanillin diffuses away from the reactive boundary layer, leading to higher yield.

Reference:

1. H. D. Thi, K. V. Aelst, S. V. d. Bosch, R. Katahira, G. T. Beckham, B. F. Sels, K. M. V. Geem, *Green Chem.,* 2022, **24**, 191-206.
2. A.Sluiter, B.Hames, R.Ruiz, C.Scarlata, J.Sluiter, D.Templeton, D.Crocker, Determination of structural carbohydrates and lignin in biomass, National Renewable Energy Laboratory, August, 2012.
3. M. Schmal, "Kinetic of reactions" in *Chemical reaction engineering*, CRC Press, Oxfordshire, 2014.
4. F. M. Casimiro, C. A. E. Costa, C. M. Botelho, M. F. Barreiro, A. E. Rodrigues, *Ind. Eng. Chem. Res.,* 2019, **58**, 16442-16449.
5. A. Galgano, C. D. Blasi, *Combust. Sci. Technol.,* 2005, **177**, 279-303.
6. B. Zaidman, H. Wiener, Y. Sasson, *Int. J. Hydrogen Energy*., 1986, **11**, 341-347.
7. Y. T. Zhu, Y. H. Liao, L. Y. Lu, W. Lv, J. Liu, X. B. Song, J. C. Wu, L. Li, C. G. Wang, L. L. Ma and B. F. Sels, *ACS Catal.*, 2023, 13, 7929-7941.
8. O. NOVOtNý, K. CeJpeK, J. VelíšeK, *Czech J. Food Sci*., 2008, **26**, 117-131.
9. J. Rencoret, G. Marques, A. Gutiérrez, L. Nieto, J. J. Barbero, Á. T. Martínez, J. C. d. Río, *Ind. Crops. Prod*., 2009, **30**, 137-143
10. J. J. Zeng, G. L. Helms, X. Gao, S. L. Chen, *J. Agr. Food Chem*., 2013, **61**, 10848-10857.
11. T. M. Liitiä, S. L. Maunu, B. Hortling, M. Toikka, I. Kilpeläinen, *J. Agr. Food Chem.,* 2003, **51**, 2136-2143.
12. Y. D. Li, T. Akiyama, T. Yokoyama, Y. Matsumoto, *Biomacromolecules,* 2016, **17**, 1921-1929.
13. R. M. B. O. Duarte, A. M. S. Silva, A. C. Duarte, *Environ. Sci. Technol.,* 2008, **42**, 8224-8230.
14. N. DiDonato, P. G. Hatcher, *Org. Geochem.,* 2017, **112**, 33-46.